



HAL
open science

FACIES PARTITIONING AT REGIONAL AND FIELD SCALES IN THE BARREMIAN KHARAIB-2 CARBONATES, UAE

Pierre Gatel, Jean Borgomano, Jeroen Kenter, Tarek Mecheri

► **To cite this version:**

Pierre Gatel, Jean Borgomano, Jeroen Kenter, Tarek Mecheri. FACIES PARTITIONING AT REGIONAL AND FIELD SCALES IN THE BARREMIAN KHARAIB-2 CARBONATES, UAE. *Journal of Petroleum Geology*, 2024, 47 (4), pp.347-372. 10.1111/jpg.12869 . hal-04730562

HAL Id: hal-04730562

<https://hal.science/hal-04730562v1>

Submitted on 11 Oct 2024

HAL is a multi-disciplinary open access archive for the deposit and dissemination of scientific research documents, whether they are published or not. The documents may come from teaching and research institutions in France or abroad, or from public or private research centers.

L'archive ouverte pluridisciplinaire **HAL**, est destinée au dépôt et à la diffusion de documents scientifiques de niveau recherche, publiés ou non, émanant des établissements d'enseignement et de recherche français ou étrangers, des laboratoires publics ou privés.



Distributed under a Creative Commons Attribution 4.0 International License

FACIES PARTITIONING AT REGIONAL AND FIELD SCALES IN THE BARREMIAN KHARAIB-2 CARBONATES, UAE

Pierre Gatel^{1,2,*}, Jean Borgomano^{2,3}, Jeroen Kenter¹
and Tarek Mecheri¹

Carbonates in the Lower Cretaceous (Barremian to early Aptian) Kharai b Formation are reservoir rocks at giant oil fields in the UAE and Qatar. The Barremian Kharai b-2 member (K60), the focus of this study, is in general composed of a regionally continuous succession of high-energy, shallow-water limestones bounded above and below by “dense” low-energy mud-rich strata. Despite several decades of research, conventional carbonate facies classification schemes and resulting facies groupings for the Kharai b-2 member have failed to show a statistically acceptable correlation with core- and log-derived petrophysical data. Moreover, sedimentary bodies potentially responsible for dynamic reservoir heterogeneities have not clearly been identified. This paper proposes a standardized facies classification scheme for the Kharai b-2 carbonates based on vertical facies proportion curves (VPCs) and variogram analyses of core data to construct stratigraphic correlations at both field and regional scales. Data came from 295 cored wells penetrating the Kharai b-2 member at ten fields in the on- and offshore UAE. Thin, dense intervals separating reservoir units were adopted as fourth-order transgressive units and were used for stratigraphic correlation. Field-scale probability maps were used to identify sedimentary bodies such as shallow-water rudistid shoals.

Regional stratigraphic correlations of the Kharai b-2 member carbonates based on the VPCs identified variations in depositional environments, especially for the lower part of the reservoir unit; depositional facies at fields in the SE of the UAE were interpreted to be more distal compared to those at offshore fields to the NW. At a field scale, the VPCs failed to identify significant lateral variations in the carbonates. However, variogram analyses of cored wells showed spatial concentrations of specific facies in the inner ramp domain which could be correlated with high-energy depositional bodies such as shoals dominated by rudist debris. The bodies were sinusoidal in plan view with lengths of up to 8 km and widths of ca. 1 km. Although similar-shaped bodies with these dimensions have been reported from other carbonate depositional systems, they have not previously been reported in the Kharai b Formation. At a regional (inter-field) scale, the stratigraphic correlation of standardized sedimentary facies remains problematic; however, mapping of facies associations and their relative proportions relative to their environments of deposition demonstrated new patterns for the stratigraphic architecture of the Kharai b-2 member in the UAE.

¹TotalEnergies, Avenue Larribau, 64000 Pau, France.

²Centre Européen de Recherche et d'Enseignement de Géosciences de l'Environnement CEREGE - UM 34 Aix-Marseille Université, CNRS, IRD, Collège de France, INRAE, OSU Institut Pythéas, BP80, 13545 Aix en Provence, CEDEX 04, France.

Key words: depositional facies, carbonates, reservoir characterization, Kharai b-2 member, Thamama Group, rudist shoal, Lower Cretaceous, Kharai b Formation, UAE.

³Carbonate Chair TotalEnergies - AMIDEX, Aix-Marseille University, TotalEnergies 64000 Pau, France.

*corresponding author, pierre.gatel59@gmail.com

INTRODUCTION

Shallow-water carbonates in the Lower Cretaceous (Barremian – Aptian) Kharai-2 Formation contain more than 50% of the hydrocarbon reserves of the UAE and Qatar (Carvalho *et al.*, 2011). In the UAE, numerous on- and offshore oil fields produce from this formation which is generally considered as a homogeneous reservoir composed of continuous carbonate strata. Previous authors have described the Kharai-2 reservoir in terms of a “layer-cake” stratigraphy at regional and field scales (Grötsch *et al.*, 1998; Melville *et al.*, 2004; Pittet *et al.*, 2002; van Buchem *et al.*, 2002, 2010; Hillgärtner *et al.*, 2003; Strohmenger *et al.*, 2006; Ehrenberg *et al.*, 2015; Al-Mansoori *et al.*, 2008; Tendil *et al.*, 2022). An underlying assumption for most of these studies was that sedimentary facies patterns can be predicted from core and log data, allowing facies distributions across and among fields to be reconstructed. However, this assumption may not take sufficient account of the role of diagenesis, which may modify both pore systems and rock types (e.g. Francesconi *et al.*, 2009; Skalinski *et al.*, 2009). Hybrid reservoir models have mixed depositional and diagenetic drivers that typically cross-cut stratigraphy (e.g. Rebelle *et al.*, 2005; Jeong *et al.*, 2017).

In addition, uncertainties are frequently associated with conventional sedimentological or depositional models and with core descriptions, classifications and the grouping of sedimentary facies and coding practices (see Galluccio *et al.*, 2022). Facies coding for shallow-water carbonates should be systematic and consistent, but an important source of uncertainty is likely to originate from the conversion of present-day surface depositional settings to the spatial partitioning of facies in the subsurface, although nearby outcrops may provide some guidance.

This paper addresses some of these issues by investigating depositional facies in the Barremian Kharai-2 member carbonates in 295 cored wells in ten oil fields on- and offshore the UAE (Fig. 1). While Strohmenger *et al.* (2006) used the term “lithofacies” (LF) to differentiate depositional rock types, in this paper we use the term “sedimentary facies” (SF) which more accurately describes the depositional attributes of a rock type and which is more commonly used in the public domain (Table 1). Uncertainties in sedimentary facies coding and depositional models are discussed and a homogenized facies model is proposed at regional, reservoir and field scales. Facies partitioning is analyzed with vertical proportion curves (VPCs) of standardized sedimentary facies in the ten fields studied (Fig. 1), resulting in probability maps showing the possible occurrence of depositional bodies such as shallow-water shoals within specific stratigraphic intervals. A new regional-

scale sequence stratigraphic framework is proposed for the study area in the on- and offshore UAE.

The aim of the present paper is therefore to establish a new stratigraphic correlation and facies partitioning scheme for the Kharai-2 member carbonates at both regional and field scales. These stratigraphic and sedimentary facies models will allow improved comparison of the dynamic behavior of the reservoirs and address the problematics of high permeability layers (Ehrenberg, 2020b). Furthermore, the models will provide a basis for understanding the role of diagenesis in controlling reservoir behavior at a field scale (c.f. Ehrenberg *et al.*, 2016; Paganoni *et al.*, 2016).

Geological Setting and Depositional System

The Kharai-2 member (previously referred to as the Thamama B: Fig. 2, Ehrenberg *et al.*, 2020a) corresponds to the middle part of the Thamama Group which includes three limestone reservoir intervals: the basal Kharai-1 (lower Barremian), the Kharai-2 (upper Barremian), and the Shu’aiba-1 (lower Aptian) (Strohmenger *et al.*, 2006; van Buchem *et al.*, 2010). Regional seismic sections show the lateral continuity of the Kharai-2 member, with no major offset by faults or unconformities (Alsharhan and Scott, 2000). The Thamama Group succession exhibits an apparently “layer-cake” stratigraphy across the UAE, reflecting the epeiric marine setting of the stable SE Arabian Plate during the Early Cretaceous (Grötsch *et al.*, 1998; van Buchem *et al.*, 2002; Al-Mansoori *et al.*, 2008; Vahrenkamp *et al.*, 2015; Ehrenberg *et al.*, 2019; Ehrenberg *et al.*, 2024, *in press*).

The Kharai-2 member corresponds to the K60 third-order tectonostratigraphic sequence of Sharland *et al.* (2001) (Fig. 2). The K60 and K70 sequence boundaries have been given different ages by different authors including Azer and Toland, 1993; Boichard, 1994; Sharland *et al.*, 2001; Davies *et al.*, 2002; van Buchem *et al.*, 2002, 2010; Granier *et al.*, 2006; Strohmenger *et al.*, 2006; Simmons, 2007; and Tendil *et al.*, 2022. The nomenclature of Strohmenger *et al.* (2006) is used here although it is subject to future revision (Galluccio *et al.*, 2022; Tendil *et al.*, 2022). Thus, the base of the K60 sequence corresponds to the top of the Kharai-1 member, and the top of the sequence corresponds to the base of the Hawar member at the K70 sequence boundary (Fig. 2). In the middle of the K60 sequence / Kharai-2 member is the K60 maximum flooding surface (K60 MFS).

The Kharai-2 member is composed of a lower “dense” interval (“Type 1 Dense”: Grötsch *et al.*, 1998) and an upper reservoir interval. These intervals are interpreted to represent deeper- and shallower-water carbonate platform environments respectively (Grötsch *et al.*, 1998). The reservoir interval is divided into six

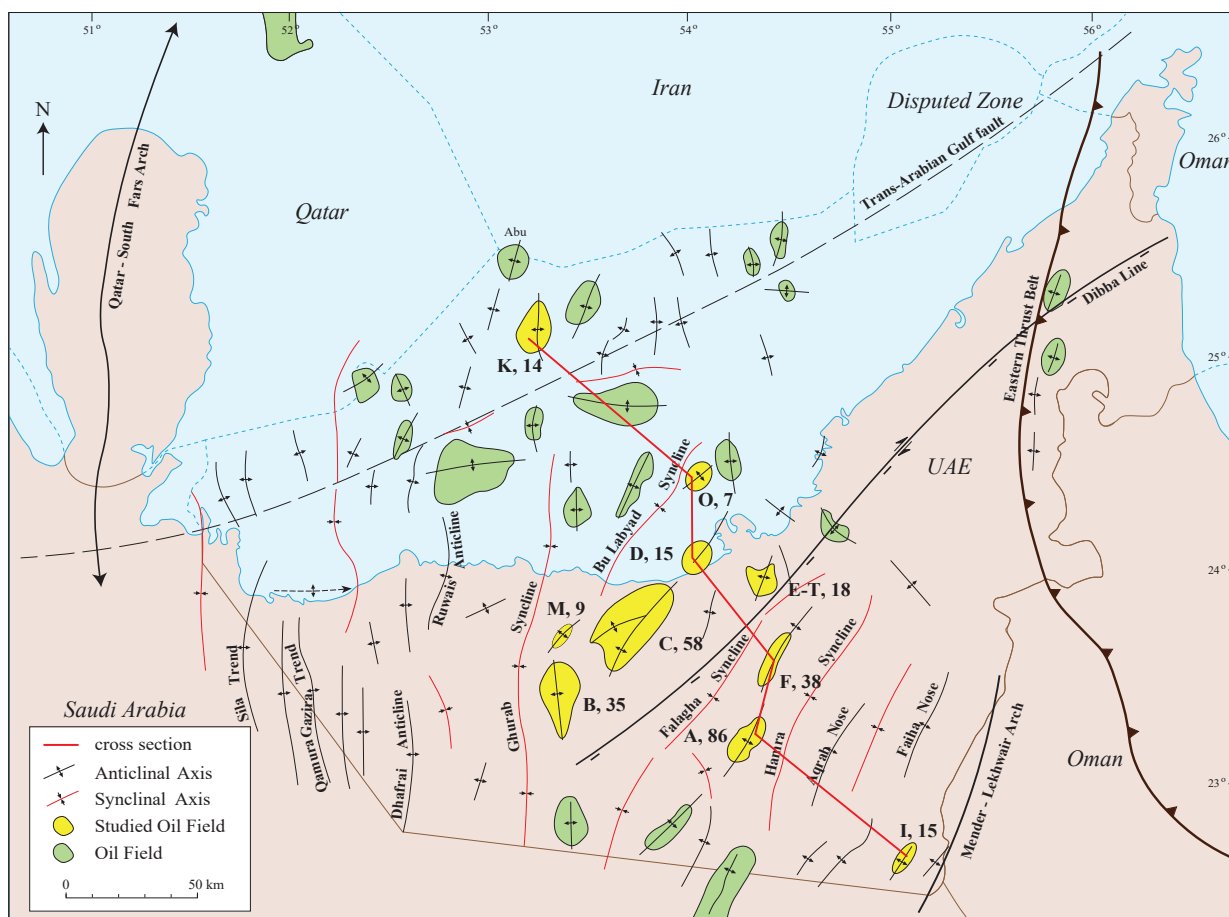


Fig. 1. Map of the UAE and the adjacent offshore area showing the locations of the ten oilfields (green ovals) producing from the Kharai2 member studied and for which vertical facies proportion curves (VPCs) were available. Fields are identified by letters; numbers indicate the number of cored wells per field. Red line is the profile of the stratigraphic correlation panel in Fig. 4a.

reservoirs units or sub-zones (Ehrenberg *et al.*, 2018; Ehrenberg *et al.*, 2020b) which are bounded by thin, low-porosity intervals referred to as “Types 2 and 3 Dense” by Grötsch *et al.* (1998).

The lower part of the Kharai2 member, which is in general interpreted to correspond to early transgressive systems tract deposits (Fig. 2), is mainly composed of *Orbitolina*-rich, deeper-water, low-energy, peloid-rich wackestones and mudstones. The depositional environments of *Orbitolinids* are not clear as they can occur in a range of specific palaeoenvironments (Masse, 1991; Leonide *et al.*, 2012); however for this study the *Orbitolina*-rich facies were interpreted as a deeper-water deposit (Masse and Fenerci-Masse, 2011; Michel *et al.*, 2023).

These dense, low porosity argillaceous limestones are burrowed and bioturbated, with high GR values which can be correlated at both the field scale (Fig. 2) and at a regional scale (Al Mansoori *et al.*, 2008). The upper part of the member (highstand systems tract) contains heterogeneous, shallow-water, high-energy carbonates with grain-supported textures (van Buchem *et al.*, 2002; Strohmenger *et al.*, 2006). Reservoir

intervals are separated by dense layers containing abundant stylolites which indicates a strong diagenetic influence (Ehrenberg *et al.*, 2016; Paganoni *et al.*, 2016). The stylolites can be correlated across the entire onshore UAE (Al-Mansoori *et al.*, 2008), suggesting a large-scale depositional and stratigraphic control on their development. Stylolite formation may have been facilitated by the presence of detrital clays, and clay supply to the Kharai2 carbonate platform may have varied over time due to sea-level oscillations or climatic and environmental changes (Ehrenberg *et al.*, 2018). The intensity of late diagenetic transformations can be correlated with the distribution of water and hydrocarbon fluids in the Kharai2 reservoirs of producing structures. Oil charge may have resulted in the early preservation of reservoir quality in up-dip locations (Strohmenger *et al.*, 2006). Tilting of the platform during the Late Cenozoic (McGeer *et al.*, 2020) may have caused further changes in fluid distribution and reservoir diagenesis.

In the study area in the UAE (Fig. 1), the main source rock is the Upper Jurassic Hanifa Formation (Khan *et al.*, 2018). Oil migration occurred during

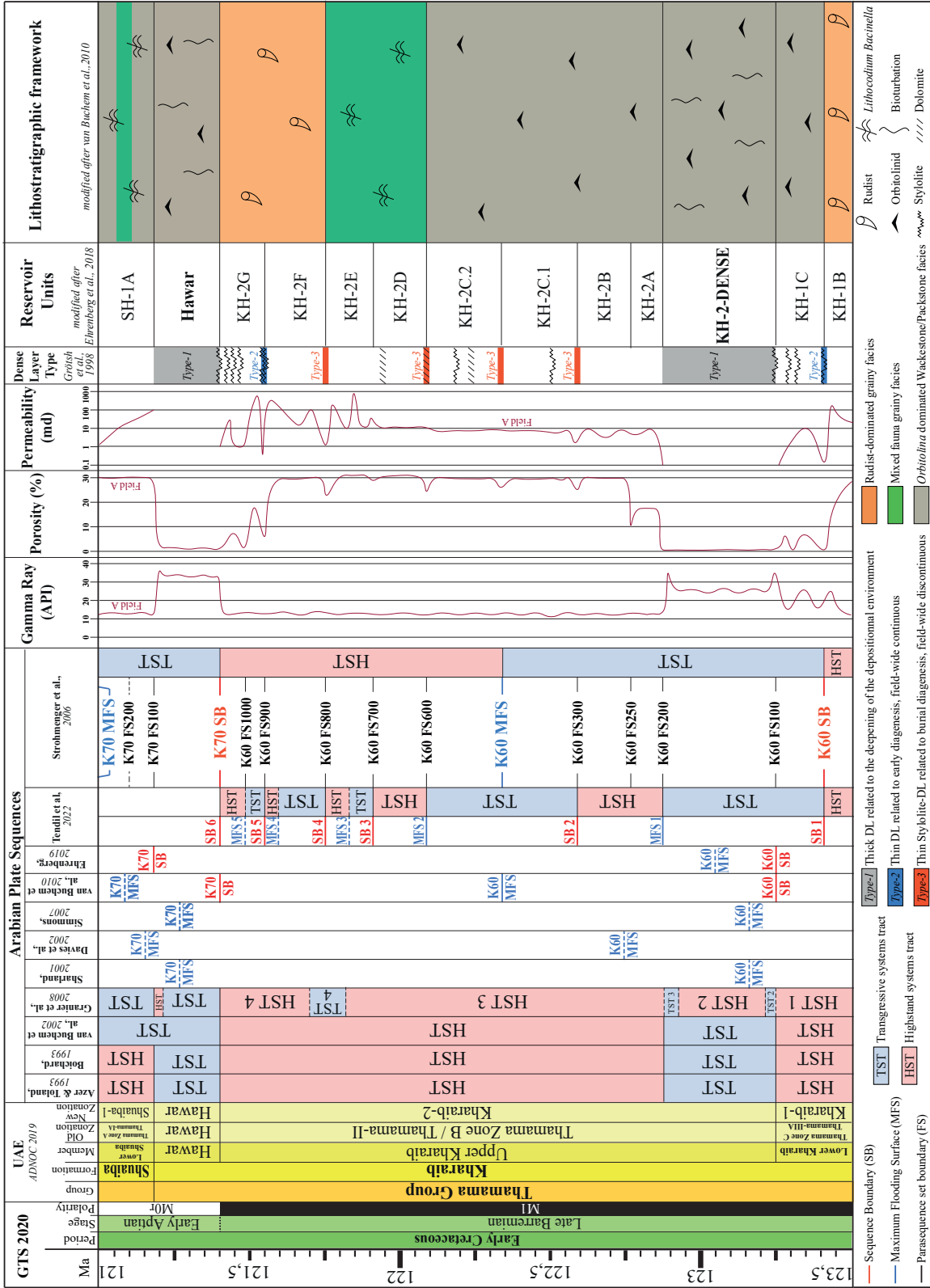


Fig. 2. Stratigraphic nomenclature for the Early Cretaceous (Barremian) Kharab 2 member in the study area in the UAE. Stratigraphic divisions and sequences are according to the authors listed in the figure. Wireline logs are updated after Strohmenger et al. (2006); reservoir units use the nomenclature defined by ADNOC, 2019.

Table 1. Facies (SF) classification and interpretation, grouped after the lithofacies defined by Strohmenger et al. (2006). Environments of deposition (EoDs) are given for each facies. Facies groupings are based on dominant biological components, sedimentary features and overall consistency with the DoE.

Facies grouping		New facies group	SF dominant environment (DE)	Zone
Lithofacies description (after Strohmenger et al., 2006)				
Facies code UAE	Complete facies name			
LF1 - RPR	Rudist, peloidal rudstone	SF1	Lagoon	Reservoir Zone
LF2.b - RPP	Rudist, peloidal packstone	SF2	Lagoon	
LF2 - RPF	Rudist, peloidal floatstone	SF3	Lagoon	
LF3.b - MPP	Miliolid, peloid packstone			
LF3 - SPP	Skeletal, peloid packstone			
LF4.b - MPG	Miliolid, peloid grainstone			
LF4 - SPG	Skeletal, peloidal grainstone	SF4	Shoal	
LF5 - CgSG	Coated-grain, skeletal grainstone			
LF6 - CgASR(F)	Coated-grain, algal, skeletal rudstone-floatstone	SF5	Shoal	
LF7.b - ASPP	Algal, skeletal, peloid packstone			
LF7 - ASPF(R)	Algal, skeletal, peloid floatstone-rudstone			
LF8 - ASFB	Algal, skeletal, floatstone-boundstone			
LF9 - OSP	Orbitolinid, skeletal packstone	SF6	Slope	Dense Zone
LF11 - OSW	Orbitolinid, skeletal wackestone	SF7	Basin	
LF10 - SPWP	Skeletal, peloid wackestone-packstone			
LF12 - SW	Skeletal wackestone			
LF13 - FSW	Foraminiferal, skeletal wackestone	SF8	Basin	
LF20 - WBSP	Wispy-laminated, burrowed, skeletal packstone			
LF23 - WBSW	Wispy-laminated, burrowed, skeletal wackestone	SF9	Basin	
LF24 - BBSP	Burrowed, bioturbated, skeletal packstone			
LF27 - BBSW	Burrowed, bioturbated, skeletal wackestone-mudstone	SF10	Slope	
LF21 - WBOSP	Wispy-laminated, burrowed, orbitolinid skeletal packstone			
LF25 - BBOSP	Burrowed, bioturbated, orbitolinid skeletal packstone			
LF22 - WBOSW	Wispy-laminated, burrowed, orbitolinid skeletal wackestone			
LF26 - BBOSW	Burrowed, bioturbated, orbitolinid skeletal wackestone			

[SF] Sedimentary Facies nomenclature [LF] UAE Nomenclature (Strohmenger et al., 2006)

Late Cretaceous regional compression which resulted in the development of anticlinal traps where oil is reservoired in the Kharai-2 carbonates (Sharland et al., 2001; Filbrandt et al., 2006). More than 15 oilfields producing from this reservoir, mostly located offshore, are located in the study area (Fig. 1) and have been in production since the 1970s.

METHODOLOGY AND DATA

At the studied oil fields (Fig. 1), the number of cored wells per fields ranges from seven (at field O) to 86 at field A. Letters used here for field identification conform to those used in previous publications (e.g. Barata et al., 2015; Ehrenberg et al., 2020a). Descriptions of cored intervals at the studied wells were provided by TotalEnergies (*unpublished data*) and include reservoir characterization studies and geological models.

To allow unbiased correlation of the Kharai-2 member across the studied fields, the first step consisted of a systematic standardization of previously-published facies groupings (Strohmenger et al., 2006, van Buchem et al., 2010) resulting in ten new groups of sedimentary facies (Table 1). This new

facies classification was subsequently applied to the 295 cored wells. A total of 27 lithofacies (LFs) in the Kharai-2 member were defined by Strohmenger et al. (2006), and 21 by van Buchem et al. (2002), based on faunal content, carbonate texture and lithological composition. In this study, we grouped together some lithofacies (2 to 4) based on their primary faunal components, sedimentary features and their dominant depositional environment (DE). Only lithofacies with the same faunal content and the same depositional environment were grouped, resulting in new composite groupings such as the coated-grain facies (SF4) and the algal facies (SF5) (Table 1). However, lithofacies with similar dominant organisms but from different depositional environments, such as the rudist-dominated LFs 1 and 2, were not grouped together (SF1 and SF2). These two lithofacies reflect differences in energy setting and depositional conditions which could result in differences in reservoir quality. Similarly, lithofacies with similar dominant organisms and the same depositional environment were not grouped if they exhibited different dominant sedimentary features; for example, lithofacies LF21 and LF22, characterized by wispy laminated and burrow features, respectively, were not grouped with lithofacies LF9 and LF11 (Table

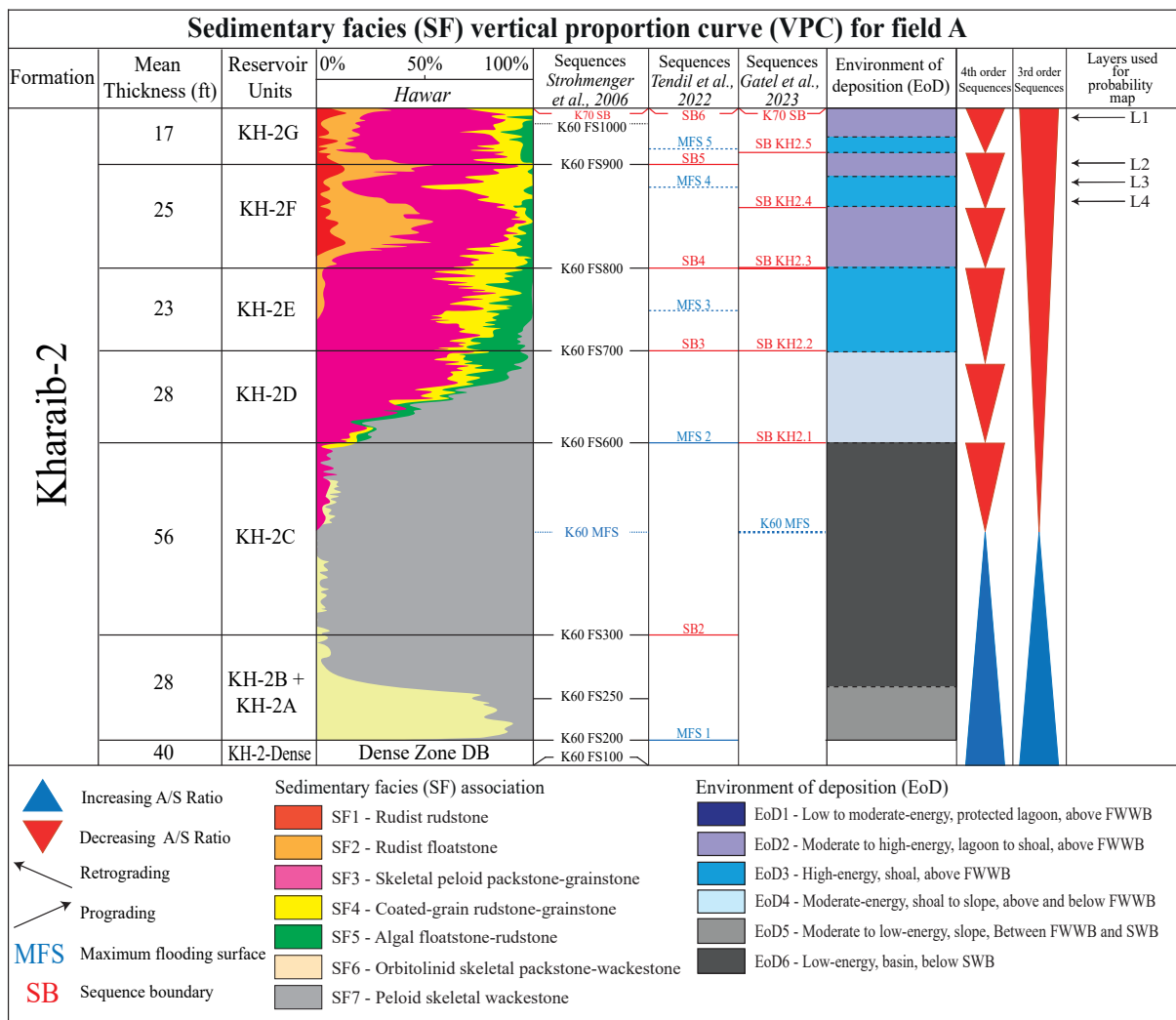


Fig. 3. Vertical proportion curve (VPC) for depositional facies in the Kharai-2 member at field A (see location in Fig. 1). The VPC shows the vertical evolution of the Kharai-2 reservoir interval with fourth-order sequences interpreted from facies variations. Key to facies colours in Table 1; environments of deposition (EoDs) are defined in Table 2. Layers 1 to 4 (L1-L4, right-most column) were used for the probability maps in Figs 8 and 9.

1). This approach ensured that the new lithofacies were not grouped based only on dominant organisms or depositional environment but that sedimentary features were also considered.

Tendil *et al.* (2022) used a different nomenclature for sedimentary facies groups in their study of the Kharai-2 interval in a field in offshore UAE. They grouped facies with similar sets of sedimentary attributes into so-called genetic elements (GEs) which also included the spatial location and shape of the depositional body, factors which may impact the depositional model.

The next step was the generation of vertical facies proportion curves (VPCs) (Deutsch *et al.*, 1996) for each field. VPCs represent variations in facies proportions over depth intervals measured from the top of the Kharai-2 member, allowing associations between depositional facies to be identified and stratigraphic trends to be estimated. This method

provided a quantitative basis for further regional stratigraphic correlations as well as geostatistical analyses and the construction of a conceptual facies model. Core coverage was approximately 70% on average for the Kharai-2 interval in the 295 wells studied; the remaining 30% was considered to have “undefined” values for facies descriptions and were not considered in the VPCs. Cut-offs and proportions of each sedimentary facies in VPCs from different fields were used to determine six Environments of Deposition (EoDs) corresponding to energy level and water depth (Table 2). In addition, local VPCs were generated at a field scale to analyze sub-field facies variations. This process was applied to fields A and F.

The last step was variogram analysis (Matheron, 1963), which was used to construct facies probability maps and to identify depositional bodies and spatial clusters or trends of particular facies. The combination of these analyses with well-section variograms allowed

more realistic depositional models to be generated. The method was applied only to field A (Fig. 1), but the depositional models could be applied to the Kharai-2 member reservoir at other fields in the UAE.

RESULTS

Facies Homogenization

The ten standardized or “homogenized” sedimentary facies (SF1 to SF10) were grouped to reflect the conventional subdivision of “reservoir” and “non-reservoir” units in the Kharai-2 carbonates. The facies groups respect the depositional environment and the lithological composition determined for each of the homogenized facies. Seven sedimentary facies, SF1 to SF7, comprise the “reservoir” zone (Fig. 3, Table 1):

SF1: high-energy, grain-supported rudist-dominated facies deposited in a shallow-water lagoon-dominated environment above fair weather wave base (FWWB).

SF2: low- to moderate-energy, grain- to mud-supported, rudist-dominated facies deposited in shallow-water, relatively protected lagoonal settings above FWWB.

SF3: low- to high-energy, grain-supported facies with miliolids, peloids and shell debris deposited in a shallow-water environment (lagoonal to shoal) above FWWB.

SF4: high-energy, grain-supported facies dominated by coated grains deposited in a shallow-water, wave-dominated shoal environment above FWWB.

SF5: low- to high-energy, grain- to mud-supported facies with *Lithocodium-Bacinella* deposited in a shallow-water, wave-dominated shoal environment above FWWB.

SF6: low- to moderate-energy, grain- to mud-supported facies dominated by Orbitolinids deposited in a shallow-water slope setting below FWWB and above SWB (storm wave base).

SF7: low-energy, mud-dominated facies with sponge spicules deposited in a basinal environment (i.e. below SWB).

Three facies (SF8 to SF10) comprise the non-reservoir or “dense” zone interval. These facies are compositionally similar to distal (below FWWB) reservoir facies, but in general have a higher clay content, lower porosity and elevated gamma ray (GR) values (Table 1, Fig. 3):

SF8: wispy laminated pack- and wackestones with sponge spicules deposited in a low-energy basinal environment below SWB.

SF9: bioturbated mud-supported pack-wackestones and mudstones with sponge spicules deposited in a low-energy basinal environment below SWB.

SF10: wispy laminated, mud-supported and bioturbated pack- and wackestones with Orbitolinids

deposited in a low- to moderate-energy slope setting below FWWB and above SWB.

Vertical Proportion Curves (VPCs) and Environments of Deposition (EoDs)

Vertical facies proportion curves illustrate variations in the average depositional facies present for cored wells in each field, as illustrated for field A in Fig. 3. Vertical facies variations may indicate vertical stratigraphic trends and sequences which can be correlated between different fields, for example along the NW-SE transect across the study area in Fig. 4a. This can be compared to the correlation of lithostratigraphic reservoir units along the same profile in Fig. 4b. The stratigraphic correlations are based on transgressive and regressive trends established from the Vertical Proportion Curves of sedimentary facies. Interpretations were based on core data from the different studied fields, with no biostratigraphy or seismic constraints.

Environments of deposition (EoDs) were defined based on variations in sedimentary facies ratios conforming to VPC motifs that occur systematically over all the fields studied in particular stratigraphic intervals (Table 2). The EoDs and the associated facies ratios are summarized below:

EoD1 is defined as a low- to moderate-energy protected lagoonal environment dominated by muddy facies and rudists, with water depths between exposure and fair weather wave base (FWWB). Facies are dominated by SF2 (rudist floatstone), proportions of which exceed 50%, which are often associated with rudist rudstones (SF1) whose proportions may exceed 25%. The rudist facies coexist with low-energy peloid wackestone-packstones (SF3, <25%).

EoD2 is defined as a moderate-energy transitional environment passing from protected lagoonal to shoal above the FWWB. It is dominated by SF3 (>30%) but other SFs are present including shoaly coated-grains (SF4) in relatively high proportions (up to 30%), *Bacinella*-rich facies (SF5, <10%) and lagoonal rudist facies (SF1, <10%; SF2 5-30%).

EoD3 is defined as a high-energy environment above FWWB. It is dominated by the high-energy grain-supported SF4 and SF5 (each between 20% and 50%). The high proportions of SF4 are however inversely correlated with SF2 which only occurs rarely (<10%). Other facies include SF3 which is present in proportions up to 50%.

EoD4 is defined as a moderate-energy environment, from shoal to slope, close to the FWWB. It can be considered as a transitional zone passing from a shoal setting (SF3, 10 to 50%; SF4 5, <20%; SF5 5-20%) to a more distal environment (SF6, 10 to 40%; SF7, 10 to 70%).

EoD5 is defined as a moderate- to low-energy slope

environment, dominated by mixed-support orbitolinid facies between FWWB and SWB. SF6 is present in proportions exceeding 70% with the more distal SF7 (<30%). In the dense interval, this EoD corresponds to high proportions of SF10 (70-100%) which coexists with low proportions of SF8 and SF9 (<30%).

EoD6 is defined as a low-energy muddy basinal environment, below SWB. It is dominated by SF7 (70-100%) in the reservoir interval, where SF6 may be present in low proportions (less than 30%). In the dense interval, this EoD corresponds to high proportions of SF8 and SF9 (70-100%) which coexist with low proportions of SF10 (<30%).

The environments of deposition were interpreted in the reservoir and dense intervals of the Kharaib 2 member according to the VPC motifs and the facies proportions (Table 2). This new classification scheme is explained below and illustrated in Fig. 3 for Field A, and was then applied to the other fields studied.

The base of the reservoir interval at the K60 FS200 horizon of Strohmenger *et al.* (2006) (Fig. 3) shows high proportions of SF6 (>70%), and the associated depositional environment is therefore interpreted as EoD5. These facies pass abruptly upwards into SF7 in proportions exceeding 70%, which is associated with EoD6. This transition to a deeper-water depositional environment indicates a transgression up to the interpreted maximum flooding surface (MFS K60) which occurs in the middle of the KH-2C reservoir sub-unit (Fig. 3). The MFS is followed by six successive regressive (probably prograding) units up to the top of the Kharaib-2 member (Fig. 3). The first of these, SB KH2.1 which ends at the top of the KH-2C sub-unit, is dominated by SF7 (>70%), a facies associated with EoD6. It is followed by the prograding SB KH2.2 sequence, occurring through the entire KH-2D sub-unit, with a gradual change of facies from SF7 (30%) to SF3 (50%), SF4 (10%) and SF5 (10%), corresponding to EoD4. A transition to the shoal-dominated EoD3 in the SB KH2.3 sequences is indicated by the occurrence of higher proportions of SF3 (<50%), SF4 (30%) and SF5 (20%). The top of SB KH2.3 marks an important sequence boundary, near the sub-dense interval between reservoir units KH-2F and KH-2E, which is followed by an alternation of facies associated with the more proximal EoD-2 and EoD-3.

The following regressive sequence (SB KH2.4) is represented by an increase in the proportion of SF2 and the appearance of SF1, corresponding to a low to moderate energy peritidal environment (EoD2). The proportions of SF1 and SF2 do not exceed 50% and therefore prevent the interpretation of EoD1. A similar alternation characterizes the above two prograding sequences, SB KH2.5 and K70 SB.









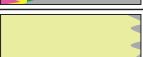



Correlation of VPCs and EoDs between fields

The VPC-based method was applied to each of the studied fields to establish the vertical facies evolution and the environments of deposition, and to investigate possible sequence stratigraphic correlations between the fields according to the principles described by van Buchem *et al.* (2002), Borgomano *et al.* (2008) and Pomar *et al.* (2015). This approach resulted in a new scheme of sequence stratigraphic correlations for the Kharaib-2 interval at a regional scale (Fig. 4a) which can be compared to the lithostratigraphic correlation of the reservoir units (Fig. 4b) (Al Mansoori *et al.*, 2008). The correlation is based on sequence boundaries and maximum flooding surfaces (SBK 60, SBK 70 and MFS K60) (van Buchem *et al.*, 2010) which roughly correspond to the top and bottom of the Kharaib-2 member. While the position of the MFS is still subject to debate, the upper and lower boundaries of the Kharaib-2 are more obvious (Fig. 4b) and are characterized by sharp contrasts in gamma ray and porosity values; similar contrasts occur within the unit between reservoir and dense intervals.

For each of the fields, transgressive and regressive phases were defined using the same principles as those used in Fig. 3 for field A and according to the vertical trends of EoDs and VPCs. This approach is similar to that used by Tendil *et al.* (2022) on field D which defined regressive and transgressive phases according to changes in faunal and clay content, texture, and factors related to hydrodynamics and cementation. It was not however supported by specific biostratigraphic or isotope analyses (Vahrenkamp, 1996). At a regional scale, the correlations in the northern fields studied (fields D to K) of the K60 sequence boundary, which determines the base of the first TST in the Kharaib 2 member, and of MFS K60, are still uncertain. Hypothetical time-lines are drawn within the sequences in Fig. 4a to illustrate the spatial evolution of the stratigraphic architecture.

The lower part of the Kharaib-2 reservoir, from the K60 SB to the KH 2.3 SB, corresponds to major NW-to-SE variations in depositional environment, particularly above the maximum flooding surface. A deepening of the EoD occurs from field K to field I as indicated by an increase in the more distal facies (SF6 and SF7). Field K, which is characterised by high proportions of the proximal *Lithocodium* - *Bacinella* and coated grain facies (SF4 and SF5), is located in offshore UAE (Fig. 1). The interpreted onlap towards the NW of MFS K60 on the top of the Dense unit in well O is hypothetical. A thick regressive trend is developed up to SB KH 2.3 and is composed of three, well-correlated, SEward prograding sequences which show overall shoaling upwards as indicated by an increase in EoDs2 and 3. A hypothetical and very subtle (few metres over 100 km) regressive wedge

Table 2. Environment of deposition (EoD) descriptions defined from VPC profiles and SF proportions. VPC signatures (in HST and TST third order sequences) are typical for the associated EoD. Each EoD is defined according to the facies proportions which are listed in the right of the table.

Environment of Deposition (EoD)	VPC Signature examples (not to scale) with field origin (A,D,F,I,K,O)	EoD Descriptions	Presence or absence of SF										Reservoir (R) vs Dense (D)
			SF1	SF2	SF3	SF4	SF5	SF6	SF7	SF8	SF9	SF10	
EoD 1	 (F)	Above FWWB, low to moderate-energy, mud-supported dominated by rudists - protected lagoon	<25%	>50%	<25%	Abs	Abs	Abs	Abs	Abs	Abs	Abs	R
	 (I)												
EoD 2	 (A)	Above FWWB, moderate to high-energy, mixed-supported peloid grainstone-packstone (GP), coated grain and algal GP and rudist F - transition lagoon to shoal	<10%	5-30%	>30%	<30%	<10%	Abs	Abs	Abs	Abs	Abs	R
	 (D)												
EoD 3	 (O)	Above FWWB, high-energy, grain-supported peloid GP, coated grain and algal GP - shoal	Abs	<5%	<50%	20-50%	20-50%	Abs	Abs	Abs	Abs	Abs	R
	 (K)												
EoD 4	 (K)	Above and below FWWB, moderate-energy, mixed-supported peloid GP, algal GP. Low proportions of Orbitolinids and Peloids PW - slope (transition shoal to basin)	Abs	Abs	10-50%	5-20%	5-20%	10-40%	10-70%	Abs	Abs	Abs	R
	 (D)												
EoD 5	 (F)	FWWB to SWB, moderate to low-energy, mixed-supported dominated orbitolinids packstone-wackestone (PW) - slope	Abs	Abs	Abs	Abs	Abs	<70%	<30%	Abs	Abs	Abs	R
	 (K)												
EoD 6	 (A)	Below SWB, low-energy slope, mud-supported dominated wackestone, below SWB - basin	Abs	Abs	Abs	Abs	Abs	<30%	<70%	Abs	Abs	Abs	R
	 (A)												

is interpreted between SB KH 2.1 and SB KH 2.2, pinching-out towards the NE between wells D and F. Despite the previously-mentioned uncertainties, there is some evidence that the lower part of the Kharai-2 reservoir (between the Lower Dense unit and SB KH 2.3) is represented by more proximal EoDs in the north (shoal-lagoon) than in the south (basin-shoal).

The upper part of the reservoir, from the KH-2.3 SB to the K70 SB, is composed of three, correlatable regressive sequences dominated by the most proximal EoDs present in the Kharai-2 member, from protected lagoonal and lagoon with abundant rudist facies (EoDs 1-2) to high energy shoal (EoD3). These three sequences may correspond to both NW- and SEward prograding units in contrast to the southwards direction of progradation of the previous interval.

Percentages of facies occurrence in the Kharai 2 member were calculated for each field studied to investigate regional facies variations. These percentages were determined separately for two stratigraphic intervals in the reservoir unit: a lower interval from the K60 SB to SB KH2.3, and an upper interval from SB KH2.3 to the K70 SB (Fig. 4b). The sedimentary facies (SFs) correspond to environments of deposition (EoDs) as defined in Table 1. Thus SF1 and SF2 correspond to EoD1, SF4 and SF5 to EoD2, SF6 to EoD3, and SF7 to EoD4. The transitional facies SF3 was present in both EoD1 and EoD2. As illustrated

in Fig. 4a, clear variations of SF proportion can be observed in the lower part of the reservoir (KH-2E to KH-2A), and the fields studied can be divided into three categories along a proximal-to-distal trend of the Kharai carbonate platform from NW to SE (Fig. 5):

“Proximal fields” (K and O) in the NW of the transect (Fig. 1) have a high proportion of SF2, SF4 and SF5 dominated by rudists, coated grains and *Lithocodium-Bacinella* facies (>75%), but low proportions of distal facies (SF6 and SF7) dominated by orbitolinids and mud (<25%).

“Intermediate fields” (B, C, D, E-T) have roughly equal proportions of the different SFs (~20 to 30% each of SF3, SF4, SF5, SF6 and SF7).

“Distal fields” (A, F, I), located in the SE of the transect in onshore UAE, have low proportions of proximal SFs (<30%) and high proportions of distal SFs (>70%).

In the upper part of the reservoir (KH-2G and KH-2F), regional trends of facies variations are not well expressed. All the studied fields are characterized by a high proportion of SF2 (rudist floatstones) and SF3 (skeletal-peloidal pack-grainstones) with some variations between fields. All the fields, except field I in the SE, can be considered as “proximal” with facies corresponding to a lagoonal environment (EoD1).

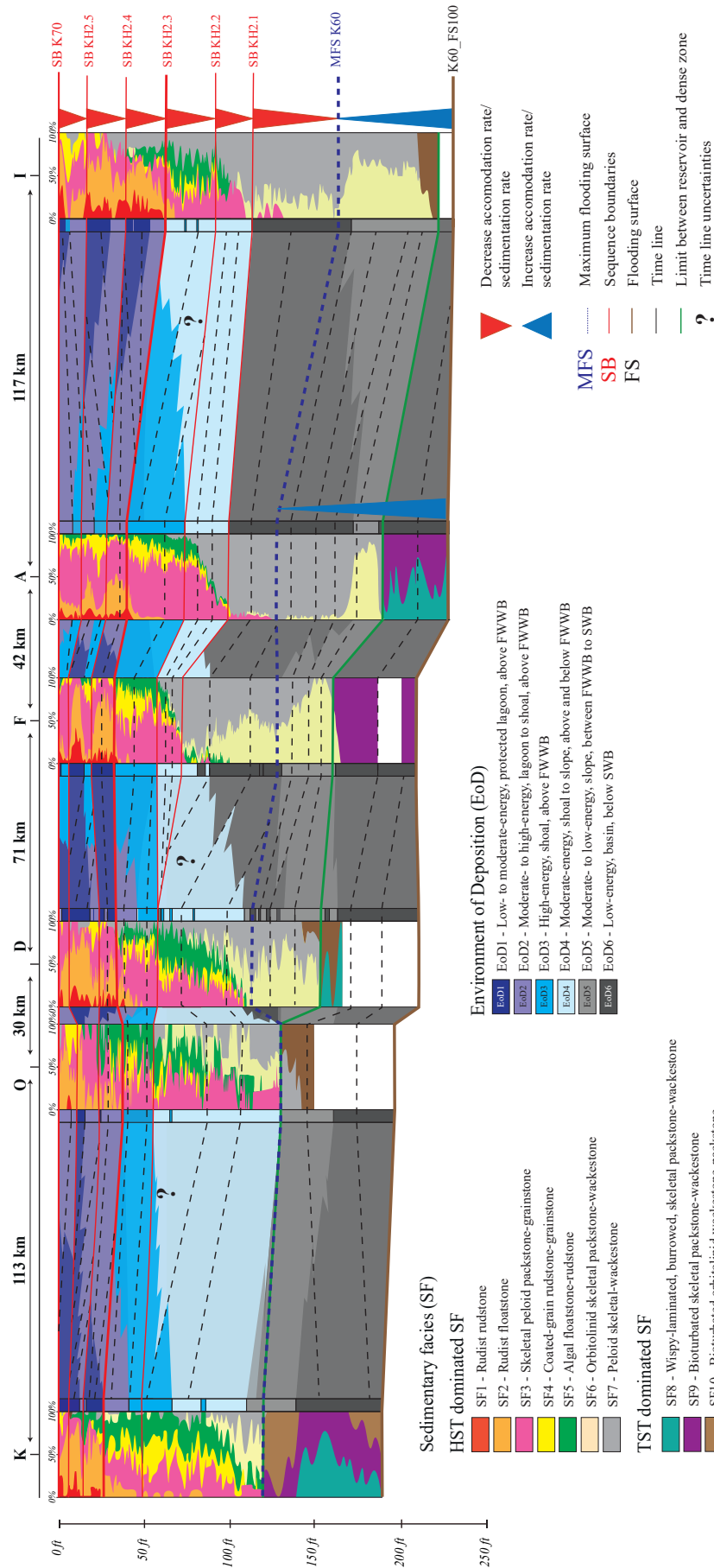


Fig. 4a. Northwest-southeast oriented sequence stratigraphic correlation panel through the study area (profile location in Fig. 1). Correlations of sequence stratigraphy and environments of deposition (EoDs) are based on vertical facies proportion curves derived from core descriptions; possible time lines are indicated by black lines. The KH2.3 SB (sequence boundary) marks the transition from the lower prograding reservoir interval (in fields K to I) to the upper, more continuous reservoir interval.

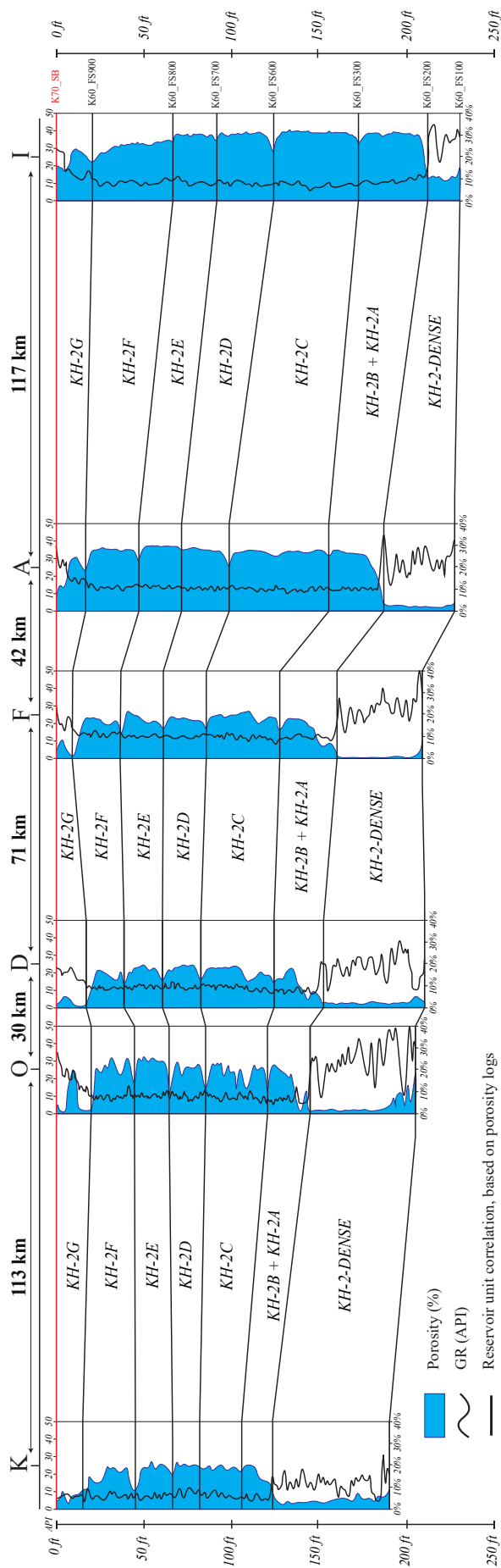


Fig. 4b. Northwest-southeast oriented lithostratigraphic correlation panel through the study area (profile location in Fig. 1) based on high-resolution log interpretations. The correlation follows that in Al-Mansoori et al. (2008) but in addition includes the K and O fields offshore and the I field onshore. Porosity is marked by blue shading, GR log profiles by black lines.

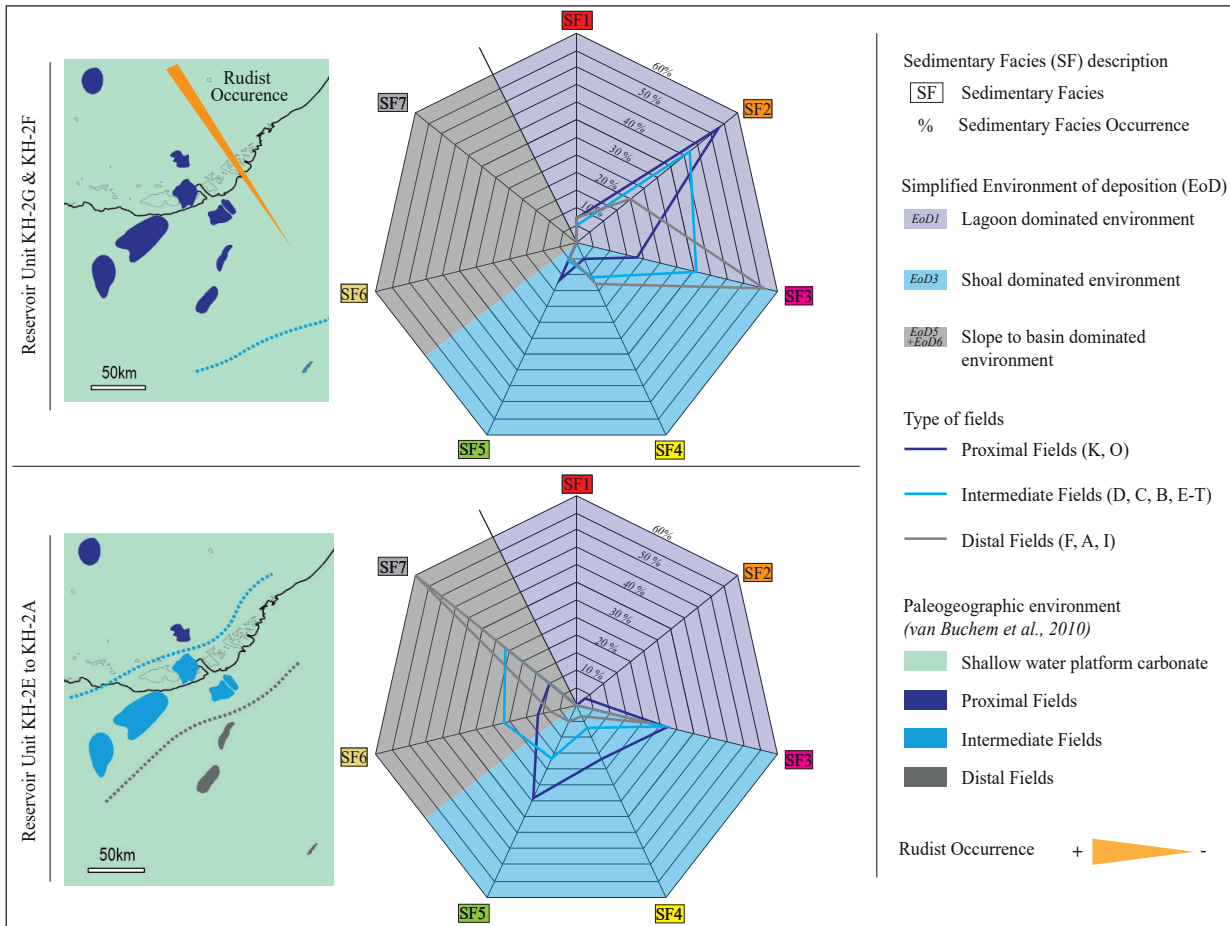


Fig. 5. Platform zonation and facies distribution diagrams for the two main reservoir intervals in the Kharai-2 member in fields in the study area: the upper interval (reservoir units KH-2G & KH-2F) and the lower (units KH-2E to KH-2A) (see reservoir units in Fig. 2). The diagrams at right show the mean facies proportions for the different fields with environments of deposition (EoDs) shown by background colours. The cartoon maps (left) show the relative locations of fields (proximal, intermediate, distal) on the Kharai platform, defined according to the facies proportions and EoD. Note the major change in facies proportions between the upper and lower reservoirs.

Facies variation at a field scale

To investigate the continuity of the stratigraphic sequences and lateral variations of EoD and facies at the field scale, VPCs from different parts of fields A and F were compared (Fig. 6). These two fields were selected as they are characterized by similar EoDs and VPCs and had high data coverage. The VPC profiles of the northern and western part of both fields were compared to those in the south and east (Fig. 6). For field A, VPC profiles in all four zones are very similar, showing the same regressive and transgressive trends defined for the entire field (Fig. 3). The facies proportion table confirms the lack of variation in facies distribution at a field scale (Fig. 6). Similar conclusions also can be drawn for field F (Fig. 6). The same stratigraphic sequences were observed in both fields. The only variations between the fields were in the relative proportions of some SFs: thus, SF2 and SF6 were more abundant in field F, and SF3 and SF7 were more abundant in field A.

To complement these field-scale investigations, a high resolution stratigraphic architecture for the Kharai-2 member in field A was established (Fig. 7). Twenty-nine cored wells were correlated on the basis of the previously interpreted stratigraphic sequences (see Figs 3 and 4) along four transects. As expected following the VPC analysis, the overall vertical succession of EoDs and the stratigraphic sequences are laterally continuous at the field scale over tens of kilometres. Lateral correlation of discrete SF layers interpreted as possible depo-bodies between wells was, however, not straightforward. Some tentative correlations of intervals dominated by rudist and grain-supported facies (SF-2, SF-4, SF-5) could be proposed locally, allowing the possible identification of metre-thick and kilometre-long sedimentary bodies. These bodies appear to conform to the overall stratigraphic architecture, and occur within a sedimentary background which is dominated by peloidal grainstone-packstones (SF3).

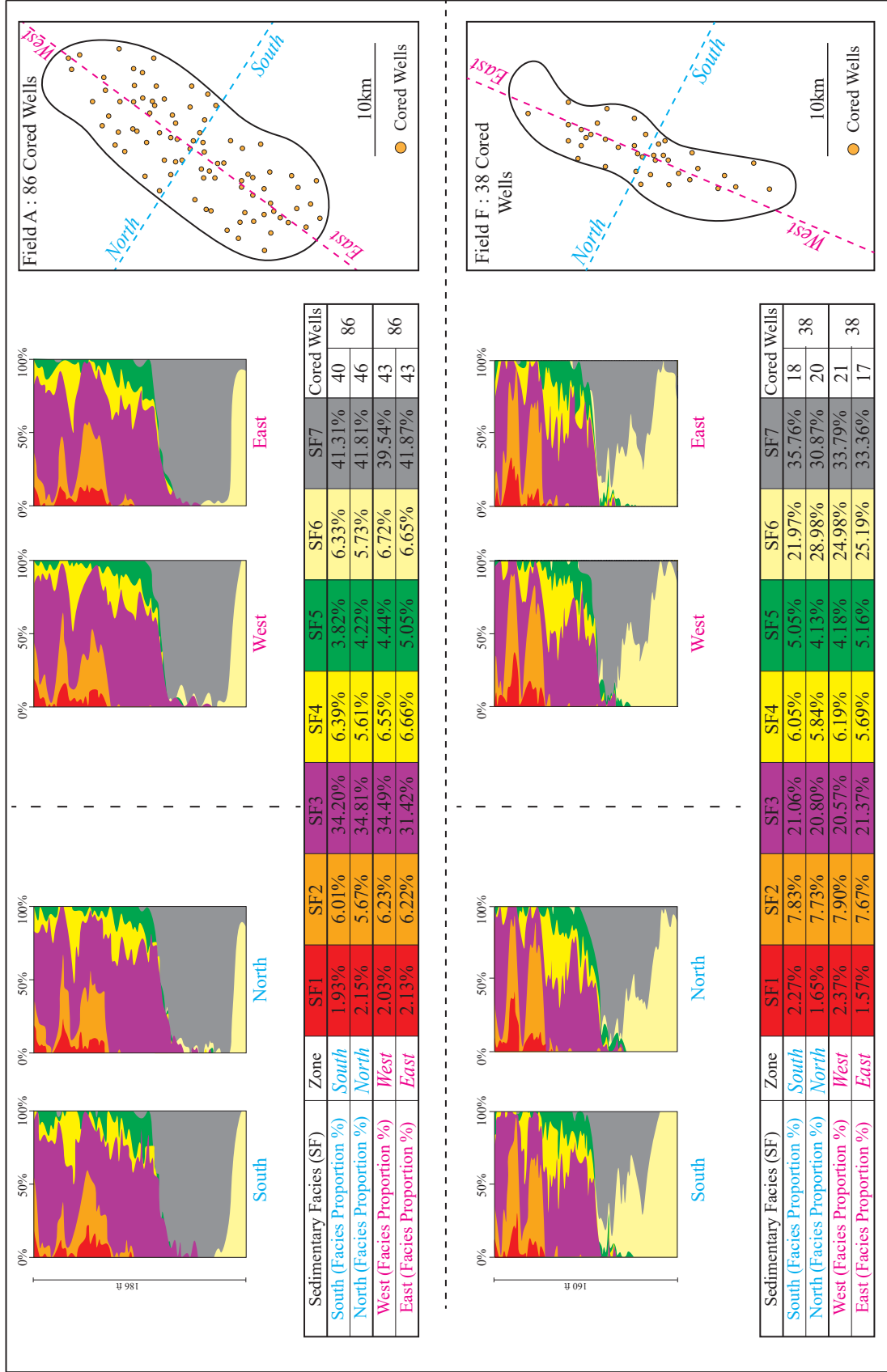


Fig. 6. Regionalized vertical facies proportion curves (VPCs) at a field scale for the entire cored section of the Kharaiib 2 member at fields A (n = 86) and F (n = 38) (see locations in Fig. 1). Facies proportions are tabulated below the VPCs. Each field is divided into four sectors (north, south, east, west) but the corresponding VPCs show no visual or statistical spatial variations.

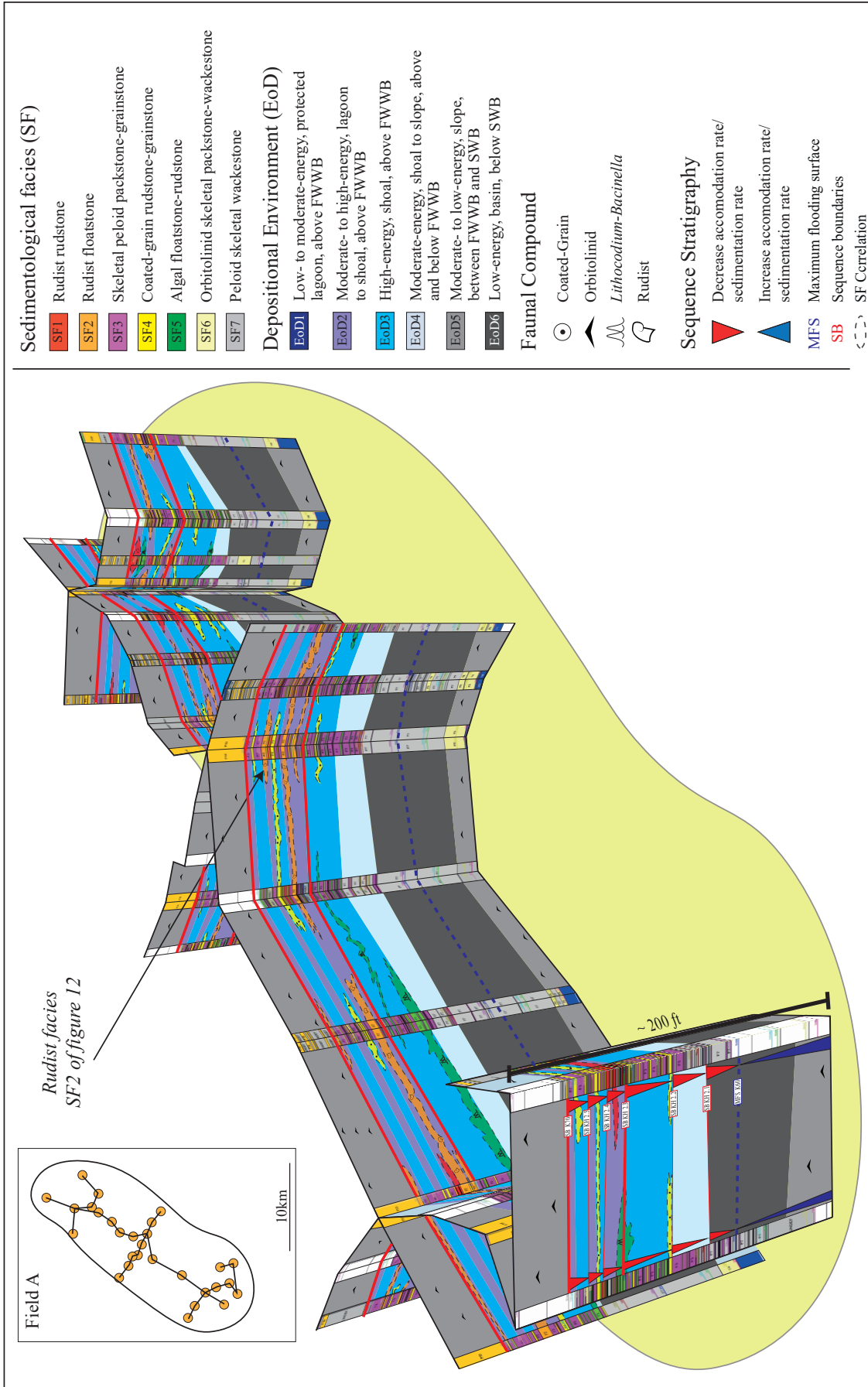


Fig. 7. Stratigraphic architecture for field A with 29 cored wells (field location in Fig. 1) based on the correlation of sequences boundaries (SBs). The K70 and KH2.3 SBs and the K60 MFS are shown (see Fig. 2), as are some interpreted sedimentary bodies.

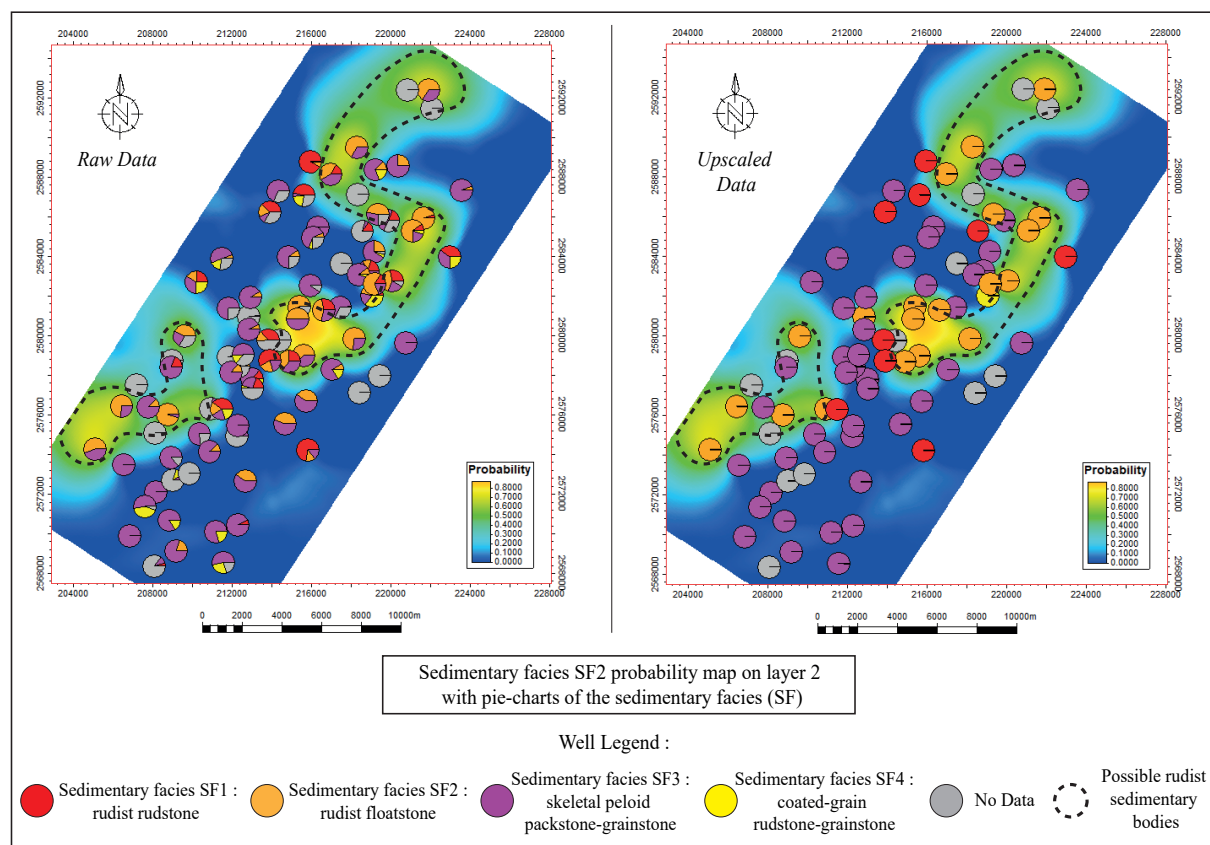


Fig. 8. Probability maps for sedimentary facies SF2 (rudist floatstone: orange circles) in reservoir interval L2 at field A. For the position of the reservoir interval, see Fig. 3; field location in Fig. 1; facies in Table 1. Maps are based on (left) raw core data and (right) upscaled data from the reservoir model. Possible rudist-rich sedimentary bodies are marked by dashed lines.

This deterministic correlation of facies intervals was complemented by geostatistical analysis of facies distributions in specific cored reservoir layers for field A (Fig. 3). The aim was to generate probability maps (Fig. 8) of facies occurrence based on the method published by Aidarbayev *et al.* (2020). Thus layer 2, located between reservoir units KH-2G and KH-2F (Fig. 3), is characterized by local patches with high concentrations of rudist-dominated facies (SF2) as illustrated by the probability map (Fig. 8). Pie-charts for the investigated layer show the facies proportions calculated in each cored well. The probability map in Fig. 8A is based on raw core facies data while the probability map in Fig. 8B corresponds to the upscaled SFs from the reservoir model. The two maps are reasonably comparable. The probability maps for facies SF2 suggest that rudist floatstone bodies are not distributed randomly at a field scale. Thus in the southern part of the field, the rudist floatstone bodies are aggregated into km-wide patches which pass into meandering/sinusoidal zones towards the north.

Probability maps showing the occurrence of SF2 (rudist floatstones) and SF4 (coated grain rudstone-grainstones) were calculated for reservoir layers L1, L3 and L4 (Fig. 9). The maps (two for facies SF2, one for SF4) show kilometre-wide patches in which there is a

high probability of SF2 and SF4 occurrence with a weak tendency to form sinusoidal zones. The probability maps indicate that rudist floatstones and coated grain rudstone-grainstones in particular reservoir layers are not distributed randomly or uniformly at the field scale, and that they may form kilometre-wide patches surrounded by peloidal grainstone-packstones (SF3).

High resolution stratigraphic correlations of cored wells near to one of the rudist floatstone patches illustrate possible patch geometry along two perpendicular 2D cross-sections flattened on the top-Hawar member (Fig. 10). The possible SF2 body is less than 2 m thick but extends laterally for over 10 km (Fig. 10b). The two cross-sections, which have a vertical scale exaggeration of $\times 10^3$, show clear lateral transitions between SF2 and the surrounding facies which mainly comprise peloidal grainstone-packstones (SF3). The flat-lying aspect of the SF2 unit over such a broad area ($>50 \text{ km}^2$) suggests the absence of erosive channels or of significant sea-floor relief due to carbonate build-ups.

Facies Models

As a result of the quantitative analyses of VPCs and SFs at both regional and field scales, conceptual facies models were established for the reservoir

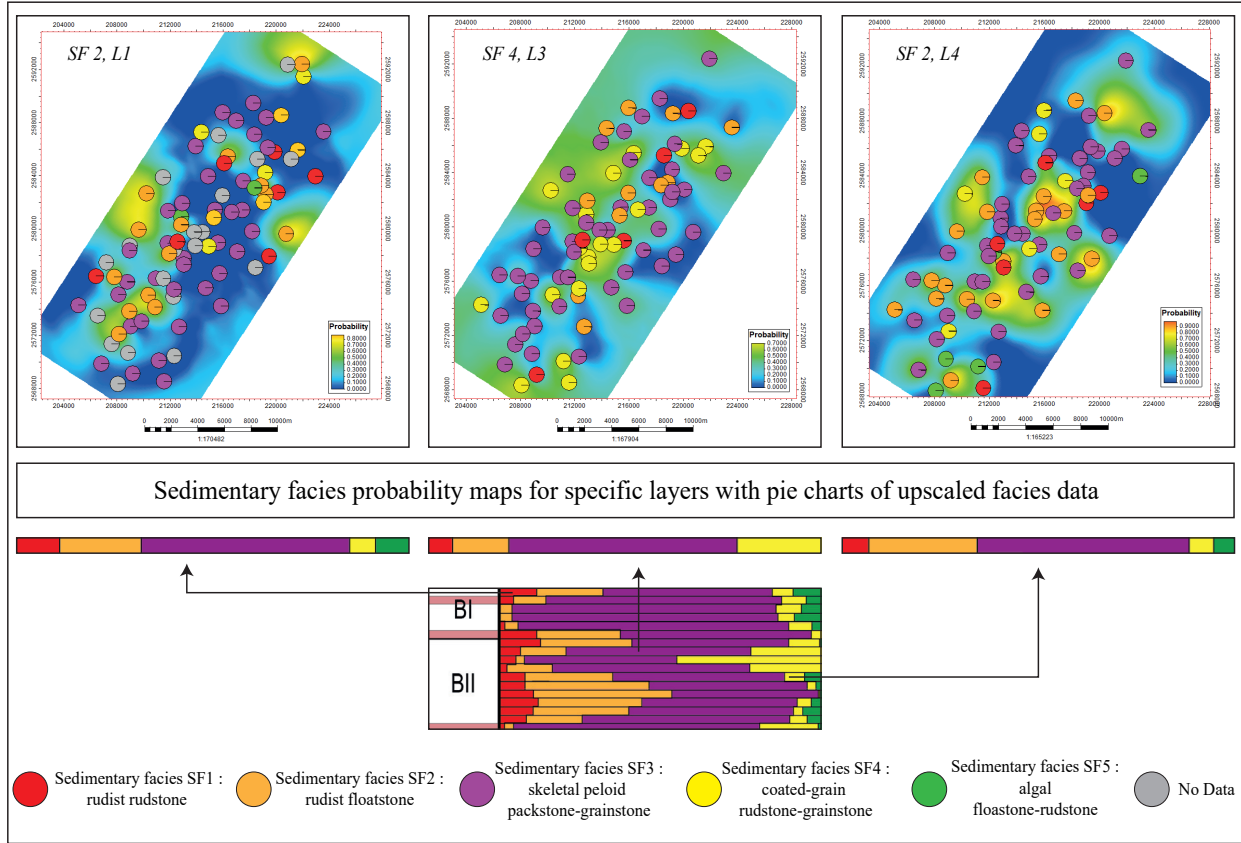


Fig. 9. Facies probability maps for reservoir intervals L1, L3 and L4 at field A, based on upscaled data from the reservoir model. See Fig. 8 caption for explanation.

and dense intervals of the Kharaib-2 member in the study area (Figs 11a and 11b). Specific VPC motifs and SF proportions (Table 2) were attributed to the six environments of deposition (EoDs) along a theoretical platform-to-basin profile which had no sharp physiographic transitions (Fig. 11a). Each of the six EoDs correspond to a range of water depths and hydraulic energies along the profile relative to wave base. Despite the on-going debate of the validity of models for ancient carbonate systems (e.g. Immenhauser, 2009; Pomar *et al.*, 2012; Purkis *et al.*, 2014), the profile represents a gradual transition from low- and high-energy shallow-water environments to deeper-water environments which is consistent with the spatial distribution of SF proportions and VPC analyses.

Fig. 11b illustrates possible facies distributions and proportions within the previously-defined EoDs. Low energy peloidal grainstone-packstones (SF3) form a continuous blanket from the lagoon to the slope and probably acted as background sedimentation for higher energy facies (SF1, 2, 4 and 5). The latter are represented by irregular and discontinuous patch-like bodies that are unconstrained by data except for the sinusoidal SF2 zones (Figs 8-10). This facies model is based on models of Recent carbonates in the Bahamas (e.g. Ginsburg, 1958; Tucker *et al.*, 1990),

on previously established facies models for Barremian carbonates in the Arabian Plate (Tendil *et al.*, 2022), and on outcrop analogues such as the Urgonian (Barremian – lower Aptian) carbonates in SE France (Arnaud-Vanneau *et al.*, 1982; Leonide *et al.*, 2012; Tendil *et al.*, 2018; Frau *et al.*, 2020; Lanteaume *et al.*, 2020; Michel *et al.*, 2023).

The facies can be divided into two main groups: pure limestones (SF1 to SF7), and clay-rich limestones (SF8 to SF10) (Table 2). Significant environmental turn-overs, suggested by alternations of these facies groups, are possibly related to climatic or sea level changes (Ehrenberg *et al.*, 2018, Lanteaume *et al.*, 2020; Tendil *et al.*, 2022).

Facies models for the “reservoir” and the “dense” intervals can be distinguished, but the dense facies model is poorly constrained and is not discussed here. The reservoir facies model represents the seven facies which occur in the reservoir zones which were deposited according to the six EoDs defined above in a mainly HST setting (Fig. 11b). The low-energy rudist-rich facies (SF1, <25%, SF2>50%), and low energy peloidal packstone-grainstones (SF3, <30%) in general occur in protected low- to moderate-energy peritidal lagoons above FWB (EoD1). The shape of facies bodies follows the results shown in Figs 8 and 9. Locally, SF1 is surrounded by SF2 probably due to

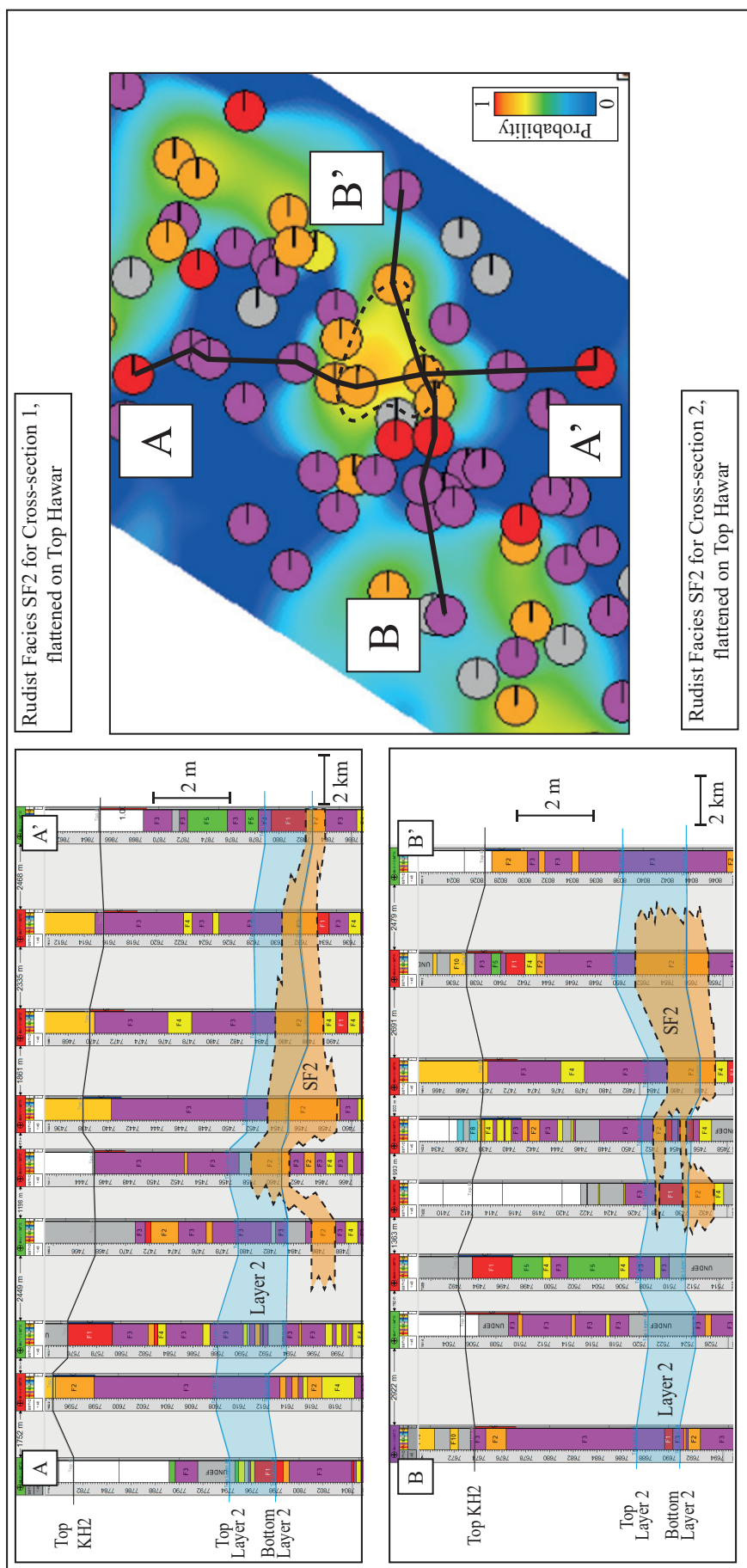


Fig. 10. High resolution stratigraphic correlations of cored wells near to one of the rudist floatstone (SF2) patches at a field scale. The two perpendicular 2D cross-sections A-A' and B-B' are flattened on the top-Hawar member (vertical exaggeration $\times 10^3$). The probability of SF2 occurrence is indicated on the figure to the right which shows the profile lines of the cross-sections. The flat-lying aspect of the SF2 unit suggests the absence of erosive channels or build-ups or other types of sea floor relief.

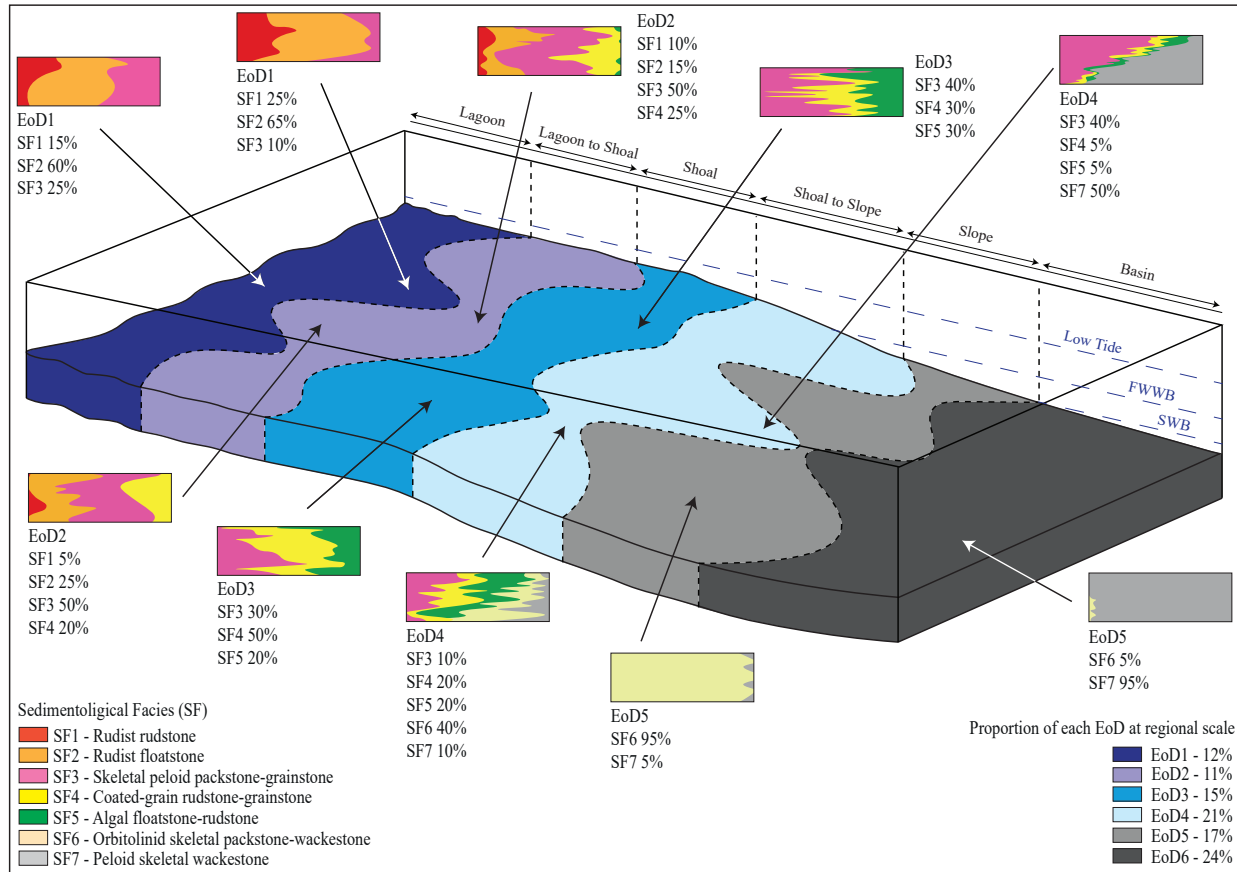


Fig. 11a. Cartoon block diagram showing the six environments of deposition (EoDs) for the Kharai-2 reservoir in the study area. EoD proportions are according to Fig. 4a. Typical vertical proportion curve (VPC) profiles are shown for facies in each EoD. Scale bar on Fig. 11b.

the disaggregation of rudstones into floatstones due to high hydraulic energies (see for example Fig. 10). SF3 (>30%) is also present in a moderate-energy, shallow-lagoon to shoal environment above FWWB (EoD2), with rare rudist rudstones (SF1, <10%), rudist floatstones (<30%), coated-grain grainstones (SF4, less than 30%), and *Bacinnella* floatstone-rudstones (SF5, <10%). SF1, SF4 and SF5, in contrast to SF2, have patchy distributions (Fig. 9). An increase in the proportions of SF4 and SF5 (20-50%) occurs in EoD3; and the appearance of distal facies (SF6 and SF7, <25%) is characteristic of EoD4, which is transitional from shoal to slope. Orbitolinid-dominated facies (SF6, >70%) are mainly present in a moderate-energy subtidal slope environment between FWWB and SWB (EoD5). It is important to note that the size and structure of the facies bodies are purely interpretative and are based only on the variograms with no support from previous studies. Finally, low-energy peloid wackestones (SF7, >70%) occur in a deeper-water subtidal slope environment below SWB (EoD6).

DISCUSSION

The discussion below focuses on the new facies and stratigraphic models for the Kharai-2 interval,

including model limitations and uncertainties, and on the models’ impact on field development compared to that of previous models.

Sedimentary Facies Coding and Depositional Models

The sedimentary facies coding used in the facies model, which grouped lithologies with similar faunal contents, is based on the sedimentological model of Strohmenger *et al.* (2006) despite the fact that it is still debated (Al-Mansoori *et al.*, 2008; Ehrenberg *et al.*, 2016, Tendil *et al.*, 2022). The differences between previously published facies models of the Kharai Formation are subtle and are not easy to replicate with available core and log data (van Buchem *et al.*, 2002; Strohmenger *et al.*, 2006; Al-Ghamdi and Pope, 2020). Lanteaume *et al.* (2020) proposed a facies classification for the Thamama Group which integrated available sedimentological data, recognizing broad, platform-scale environments corresponding to the EoDs of the present study, together with depositional facies corresponding to the SFs of the present study. As proposed by Lanteaume *et al.* (2020), separate facies models can be distinguished for the dense and reservoir units, and correspond respectively to (i) a terrigenous-influenced carbonate ramp dominated by orbitolinid

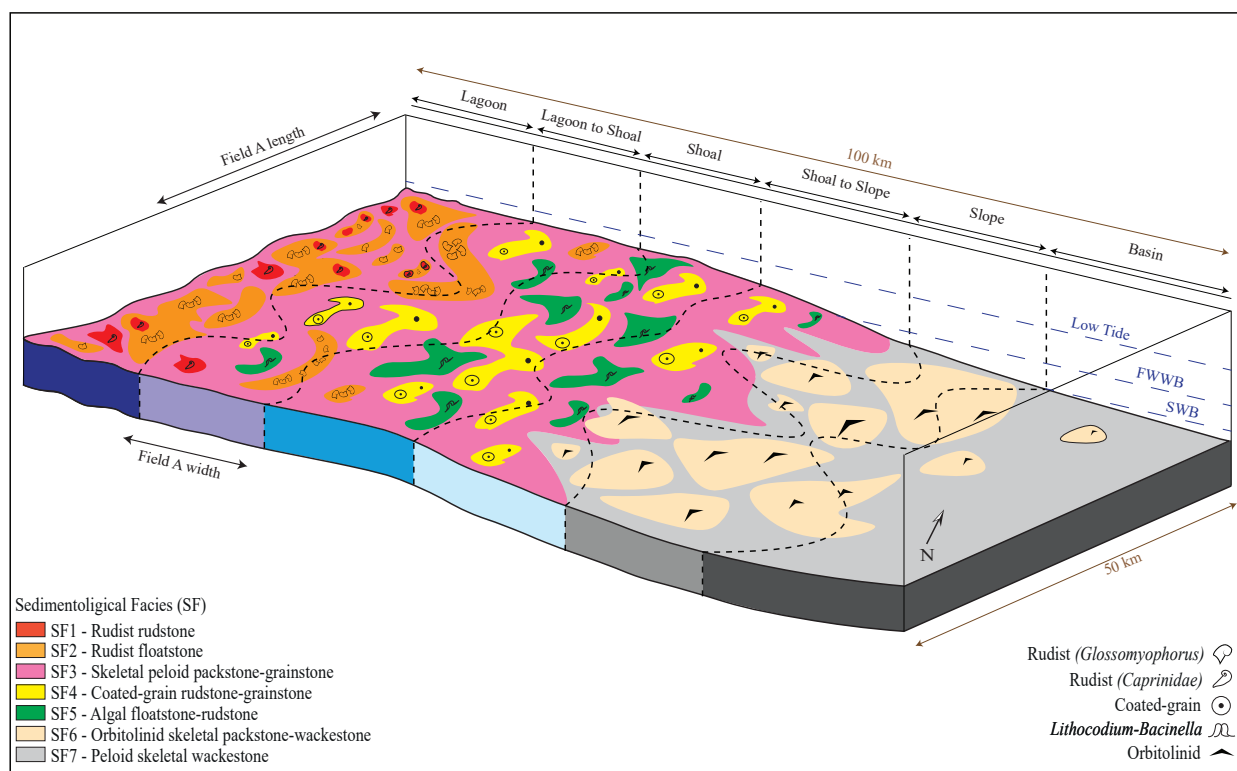


Fig. 11b. Cartoon block diagram showing environments of deposition (EoDs) for the Kharai-2 reservoir in the study area with sedimentary bodies interpreted from facies probability maps. Dashed lines represent boundaries between EoDs. Note the approximate scale bar.

fauna; and (ii) a broad carbonate platform with rudist fauna characterized by a typical long-range facies zonation related to subtle variations of bathymetry and hydrodynamics (Fig. 11).

Recent facies classifications proposed for the Kharai-2 member (Galuccio *et al.*, 2022; Tendil *et al.*, 2022) show only subtle textural and palaeo-ecological differences compared to the classification of Ehrenberg (2018). The classification of Galuccio *et al.* (2022), used by Tendil *et al.* (2022) for the Kharai-2, consisted of grouping facies by depositional environment, water depth and energy level with the support of log responses, despite the obvious difficulty of linking the latter to carbonate depositional facies. These authors' interpretative carbonate Depositional Environment (DE) scheme in general follows that used in the present paper; their DEs refer to environmental interpretations of deposits which consist of groups of lithofacies interpreted to be genetically related (i.e. deposited in the same environmental setting). In common with the EoDs of the present paper which regroup different sedimentary facies, their DEs are based on different lithofacies. By identifying the depositional environment directly from core data, the Galuccio *et al.* (2022) facies coding appears to better capture reservoir heterogeneity than the Strohmenger *et al.* (2006) lithofacies classification. In particular, abundant peloidal packstone-grainstones (SF3) were observed in the Kharai-2 member and were associated with three

different environments of deposition (EoDs1, 2 and 3). Refinement of the classification using the Galluccio *et al.* (2022) model could potentially distinguish peloidal packstone-grainstones for each facies, i.e. SF3a for EoD1, SF3b for EoD2 and SF3c for EoD3. This would lead to improved identification of EoD variations at the field scale and of variations in reservoir quality. In contrast, the current classification approach shows continuous environments of deposition at the field scale (Fig. 7).

It should be borne in mind that such carbonate facies models are conceptual and are not based on laterally continuous observations over long distances (>10 km). Also, the supporting palaeo-environmental interpretations are based on incomplete data (well cores) that are deterministically correlated (cf. discussion in Borgomano *et al.*, 2008) and spatially organized at the regional scale (Fig. 5). Possible Barremian analogue outcrops around the margins of Neotethys are similarly discontinuous and of limited extent (e.g. Everts *et al.*, 1995; Borgomano *et al.*, 2002; Bover-Arnal *et al.*, 2009; Léonide *et al.*, 2012). Despite these uncertainties and limitations, the facies and EoD models presented in this paper are broadly consistent with previous models for Kharai-2 Formation equivalents in Oman (van Buchem *et al.*, 2022; Sena and John, 2012), and Saudi Arabia (Al-ghamdi *et al.*, 2013). Advantages of the EoD model are that it is based on quantitative analyses (VPCs) which are therefore

replicable, on the regional correlation of VPC trends, and on possible evidence for coalescent rudist bodies at the field scale. This analysis therefore questions the Strohmenger *et al.* (2006) classification in quantifying field-scale reservoir heterogeneity. However, the implications of these different classifications on reservoir heterogeneity modelling are difficult to assess without petrophysical analyses from cores and log responses and without flow modelling, and these aspects will be addressed in future publications (Mangane *et al.*, *in press*; Gatel *et al.*, *in prep.*).

Regional stratigraphic correlation

As a result of the VPC analyses, a new sequence stratigraphic correlation of the Kharib-2 member has been interpreted (Fig. 4) within a chronological framework established by previous authors (Al-Mansoori *et al.*, 2008; van Buchem *et al.*, 2010). Regressive and transgressive trends were correlated at a regional scale between the fields studied, assuming that the VPC-based EoD model (Fig. 11a) can be used for the interpretation of accommodation/sedimentation (A/S) trends (but see the discussion of this problem in Borgomano *et al.*, 2008 and 2020) and in the absence of absolute age dating, biostratigraphy and seismic constraints. Despite all these uncertainties, the proposed interpretation in Fig. 4a acknowledges the fact that within the Kharib-2 interval, there occurs a significant lateral facies change from proximal to distal at regional scale.

The greatest uncertainty in stratigraphic interpretation concerns the position of MFS K60 and SB KH 2.2 between fields F and K relative to the lithostratigraphic boundary between the “dense” and “reservoir” intervals (Fig. 4a). Our interpretation implies that the lower part of the Kharib reservoir interval consists of more abundant proximal, higher energy facies (SF 3-4-5) in fields K-O-D than in fields F-A-I (SF 6-7) which could significantly impact the reservoir quality (Fig. 4a). This lateral transition affects more than one-half of the Kharib reservoir interval at a regional scale and is clearly expressed by the progradation of the platform towards the SE (Figs 4b, 5). This progradational trend is correlated to an increase in the thickness of the reservoir interval, which was probably controlled by increasing subsidence associated with the future development of the intrashelf Bab Basin in this region (Scott, 1990; Masse *et al.*, 1997; van Buchem *et al.* 2002). Correlation based on porosity log responses (Fig. 4b) alone does not allow such an identification of stratigraphic patterns and lateral depositional facies variations. Among future challenges will be to identify the impact of diagenetic overprints and to work out the relationships between rock properties, depositional facies and stratigraphic architecture (Grötsch *et al.*, 1998, Ehrenberg *et al.*,

2016, Paganoni *et al.*, 2016, Ehrenberg *et al.*, 2024, *in press*).

The new model questions the position of the MFS K60 (Fig. 2) and the inverse thicknesses of the “dense” “reservoir” units. Strohmenger *et al.* (2006) placed the MFS at the position of the greatest water depth associated with muddy wackestone facies; while Tendil *et al.* (2022) interpreted the MFS as occurring at the transition between the argillaceous dense unit and the non-argillaceous reservoir unit, highlighting the change in environmental conditions which were possibly related to a sea level rise (Ehrenberg *et al.*, 2018). The position of the MFS in this study is equivalent to that in the stratigraphic models of Strohmenger *et al.* (2006) and van Buchem *et al.* (2010), occurring at the point of interpreted maximum palaeo-bathymetry and not at the boundary between the reservoir and dense intervals. This interpretation proposes that the transition from the “dense” interval to the reservoir interval is not attributed to an alteration in accommodation or in sedimentary processes, but rather results from the influx of terrigenous material to the carbonate system. In fact, the distal facies SF6 and SF7 are very similar in composition to the dense facies SF8, SF9 and SF10, except for differences in the clay content. The stratigraphic correlation shows a decrease in thickness of the dense unit, while the overall thickness of the lower reservoir unit increases in the same direction. Ehrenberg *et al.* (2019) hypothesized that the presence of the dense zones was related to a regional influx of terrigenous clay. The input of terrigenous material from the NW could have been particularly significant at the beginning of the Kharib-2 sequence and gradually decreased upwards, but only impacted fields in the NW UAE. The change from a “dense” interval to a reservoir would not therefore be synonymous with a maximum flooding surface, whose most probable position would correspond to the deepest palaeo-bathymetry (Strohmenger *et al.*, 2006; van Buchem *et al.*, 2010; Ehrenberg *et al.*, 2019).

By contrast, the uppermost interval of the reservoir (above the KH 2.2 SB), which shows overall aggradation but with several relatively thin regressive sequences, does not show significant variations in thickness or in lateral facies patterns. During the regressive periods, EoDs remained proximal (EoD 1-2-3) and were dominated by rudist and grain-supported facies (SF 1-2-3), with possible changes in the direction of the short range progradations (Fig. 4a). This change of stratigraphic pattern and polarity in the uppermost reservoir interval could be related to the flatter physiography of the platform, which developed when accommodation and carbonate production had reached an equilibrium and hydrodynamics played the most important role, as illustrated on the modern Bahamas carbonate platform (Purkis *et al.*, 2019). The absence

of preserved transgressive trends is not surprising on such a shallow and flat platform where there were high carbonate production rates (Schlager, 2005; Catuneanu *et al.*, 2009; Borgomano *et al.*, 2020).

The occurrence of a stratigraphic wedge below SB KH 2.2 in the southernmost fields F, A and I also merits some discussion. This possible “forced regression” wedge is evidenced by the abrupt development of a shoal-slope (EoD 4) above the basinal EoD6. This rapid transition could be the result of a negative accommodation pulse, perhaps due to tectonic or sea level variations. However, the thickness difference of only a few metres over tens of kilometers suggests that the transition was related to local currents that created topography in the mosaic of facies rather than to a forced regressive wedge.

In summary and based on the sequence stratigraphic correlation presented above, the reservoir unit of the Kharai-2 member is composed at a regional scale of two main carbonate intervals, separated by the KH 2.1 SB, which possess distinct facies architectures: (i) a lower interval dominated by gradual facies evolution related to initial platform retrogradation followed by progradation towards the SE; and (ii) an upper interval composed of four regressive sequences with variable directions of progradation. This contrasting stratigraphic organization may have important influences on reservoir heterogeneities and properties at a field scale which will be investigated in future studies.

Sedimentary bodies in the Kharai-2 member and palaeogeography

Previously published stratigraphic correlations and facies models for the Kharai-2 member (e.g. Strohmenger *et al.*, 2006; Al Mansoori *et al.*, 2008) failed to identify genuine sedimentary bodies at the field scale. Furthermore, sedimentary bodies such as shallow-water shoals could not be identified with confidence from the high-resolution facies correlations presented in this study (Fig. 7).

Discrete sedimentary bodies analogous to those identified in modern shallow-water carbonate environments (such as shoals, patch reefs and banks: Purkis *et al.*, 2014; Harris *et al.*, 2015, 2019) may not have been preserved (or even developed) in the Barremian carbonate platform which hosted the Kharai-2 Formation. The probabilistic maps of facies occurrence suggest that meandering, coalescent patches of rudist facies may be present in specific stratigraphic intervals. When combined, these patches may delineate a sedimentary body less than 3 m thick but with a lateral extent exceeding 10 km (Figs 6–8). These dimensions are of the same order of magnitude as rudist bodies in the Barremian carbonate platform in SE France (Fenerci-Masse *et al.*, 2005). They are

however more extensive than those reported by Purkis *et al.* (2012) from the upper Albian rudist reef build-ups exposed along the Pecos River Canyon in Texas, where rudist packstone bodies have a mean extent dip of approximately 50 to 100 m. These size differences could be linked to differences in platform physiography, although the factors that controlled the organization of the sedimentary bodies are still uncertain. The absence of evidence for infilling of pre-existing topography (channels) or for sedimentary thickening (Fig. 10) supports the hypothesis of lateral facies variations on the sea floor controlled by relatively gentle wind-induced, tidal or storm-return currents operating in a broad and flat shallow-marine platform environment (Fig. 12) (Fenerci-Masse *et al.*, 2005).

The stratigraphic correlation panel (Fig. 4a) shows an increase in palaeo-bathymetry around field A, suggesting possible in-field facies bodies that could be interpreted as tidal bars similar to the Recent ooid shoals in the Bahamas near the end of the Tongue of the Ocean (Purkis and Harris, 2017; Rankey and Reeder, 2010). According to a palaeogeographic map of the Arabian Plate for the Barremian (van Buchem *et al.*, 2010), the presence of an open ocean to the NE of the A field, i.e. perpendicular to the axis of the meandering facies bodies, could indicate possible tidal or storm effects which may explain this arrangement. Similarly, contemporaneous trade winds, blowing from SE to NW, support the orientation of rudist fragments with respect to wind direction.

The regional palaeogeography in Fig. 12 attempts to combine the EoD and facies trends towards the SE within the platform interior, and the proximity of the oceanic platform margin towards the east. While the general progradational, thickening and deepening trend of the lower Kharai-2 reservoir interval towards the SE could be controlled by differential subsidence, the facies partitioning and possible elongation of the meander-shaped rudist bodies could have been influenced by hydrodynamics related to the proximity of the open ocean.

Reservoir Characterization

Kharai-2 reservoir units represent carbonate intervals with a variety of reservoir qualities (Ehrenberg *et al.*, 2020b) (Fig. 4b). Correlations of these units may be debated at a regional scale as they do not fit systematically with sequence stratigraphic correlations (Fig. 4a), but they are commonly used by the oil industry for reservoir modelling. The combination of depositional, stratigraphic and diagenetic processes may therefore result in a continuous petrophysical layering at the field scale, and this layered pattern may be repeated in all the fields studied. Independent of petrophysical analyses, the correlation of VPC and facies trends shows a similar layered pattern at the field

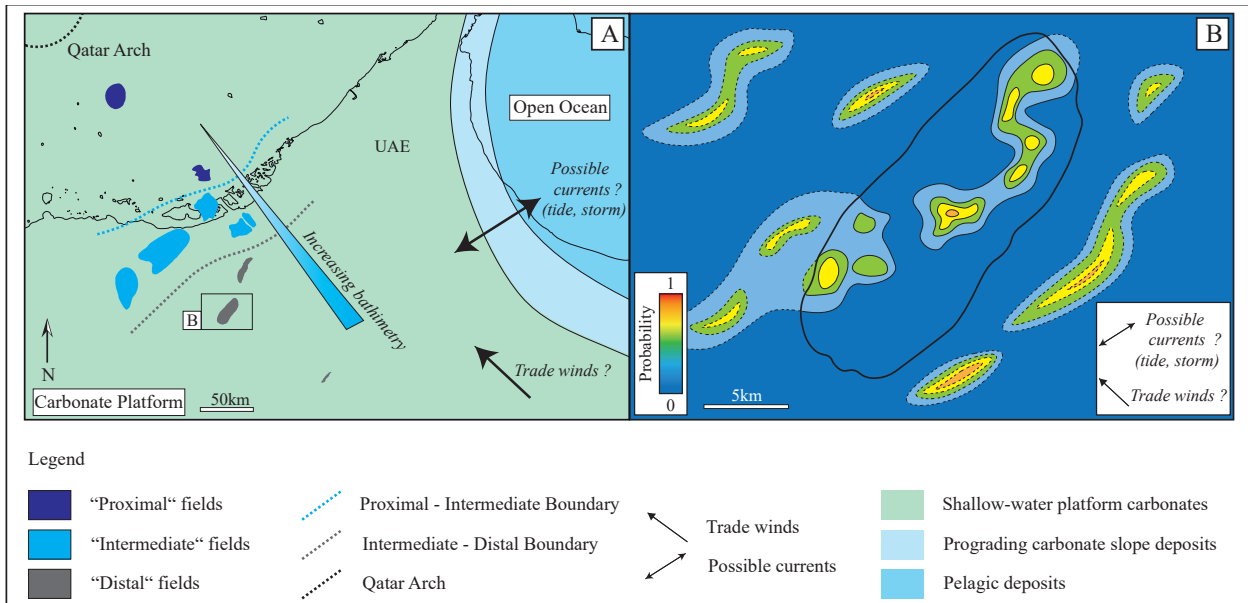


Fig. 12. Palaeogeographic maps for the Barremian Kharaib-2 member in the study region.

(A) Regional-scale map showing the location of the studied fields in on- and offshore UAE relative to the open Neotethys and the adjacent carbonate platform. Marine currents and winds could have influenced the shape and orientation of sedimentary bodies in the platform interior. Box shows the location of the map in (B). (B) Smaller-scale map of the field A area (location in Fig. 1) showing the possible shapes of SF2 bodies at a field scale according to probability maps and interpreted environmental factors influencing deposition (e.g. currents and trade winds).

scale for the EoDs (despite some significant variations in the upper part of the member), and for the overall evolution of the carbonate platform palaeo-bathymetry (Fig. 7).

The present study showed that the Strohmenger *et al.* (2006) facies model for a giant Abu Dhabi oil field failed to identify reservoir heterogeneities at the field scale. However, Galuccio *et al.* (2022) presented a facies scheme which captured heterogeneities in reservoir quality in field D in the study area (location in Fig. 1). A recent study based on log responses (Mangane *et al.*, submitted) also failed to identify a statistical relationship between reservoir rock type and facies, with reservoir quality possibly controlled more by diagenetic processes than by depositional facies. It is not straightforward to establish spatial correlations between petrophysical reservoir units and depositional environment layering at a field scale because the EoDs do not necessarily fit with the delineation of reservoir units. However, continuity of sedimentary cycles across fields and correlatable reservoir units related to diagenetic fabrics at a regional scale highlights the significant impact of stratigraphy on the reservoir architecture.

In relatively flat-lying and broad shallow-marine carbonate systems, “early” and shallow-burial diagenetic transformations and associated petrophysical modifications of carbonate sediments are often the product of shallow aquifers displacing laterally along the sedimentary profile (Moore, 1989; Tucker *et al.*, 1990). These processes and the resulting petrophysical

layering have been well described in reservoirs composed of isolated, aggrading carbonate platforms such as those at Malampaya, offshore Philippines (Fournier and Borgomano, 2007) and Yadana, offshore Myanmar (Teillet *et al.*, 2019). Similarly, stratigraphically-confined diagenetic processes and associated petrophysical layering have been observed in the Urgonian carbonate platform in SE France (Léonide *et al.*, 2014), which is time-equivalent to the Kharaib Formation. In future studies, flow modelling will be applied to identify the impact of the depositional facies model on flow behavior, and in particular to evaluate the importance of the grainy and rudistid bodies responsible for reservoir heterogeneities in the Kharaib-2 member (Jeong *et al.*, 2017; Ehrenberg *et al.*, 2020b).

CONCLUSIONS

This paper proposes a new regional-scale stratigraphic correlation for the Lower Cretaceous Kharaib 2 member in a study area on- and offshore the UAE based on the analyses of vertical proportion curves (VPCs) of standardized sedimentary facies (SFs). The correlation points to the possible occurrence of rudistid bodies which could result in significant reservoir heterogeneity at a field scale. Reservoir unit correlations based on lithostratigraphy appear to be consistent for oilfields on- and offshore the UAE where diagenetic modification is in general comparable, but they fail to capture sedimentary and stratigraphic variations at a

field scale. The stratigraphic sequences defined in this paper allow variations in depositional environment to be highlighted between fields, especially for the lower part of the Kharai 2 member reservoir interval. This part of the reservoir is dominated by relatively distal sedimentary facies at fields located in the SE of the study area in onshore UAE; whereas offshore fields located to the NW have more proximal SFs. By contrast, the aggrading, upper part of the Kharai-2 reservoir does not show significant lateral variations in thickness or facies at a regional scale. The same stratigraphic cycles are present in all the fields studied, almost all of which show the same succession of EoDs; an exception is onshore field A in the SE of the study area where the reservoir is dominated by relatively proximal EoDs.

The field-scale approach allowed the continuity of EoDs to be resolved at a small scale but failed to capture the occurrence of sedimentary bodies such as rudist shoals and build-ups. Standard correlations used in the oil industry, based on petrophysical properties related to diagenetic modifications conforming to the stratigraphic architecture, do not allow the correlation of sedimentary bodies at a field scale. Neither are these bodies captured by vertical facies proportion curves which rather show continuity in the reservoir stratigraphy of the various fields. However probability maps, based on data from 84 cored wells, suggested the occurrence of km-scale sedimentary bodies whose complexity and origin need further study. The identification of such stratigraphic variations at a regional scale, and the recognition of sedimentary bodies at a field scale, will be a key to understanding the heterogeneity of the Kharai-2 member in the study area and the controls on the reservoir's dynamic behaviour and flow properties.

ACKNOWLEDGEMENTS

The authors thank TotalEnergies and ADNOC for providing the data used for this study and for permission to publish the paper. They also thank the AMIDEX foundation (Aix-Marseille University, France) for financial support. Careful review comments by Frans van Buchem and an anonymous referee improved the paper and are acknowledged with thanks.

Data availability statement

All data used in this paper were provided by the TotalEnergies database.

REFERENCES

- AIDARBAYEV, S., PAMUNGKAS, S., AL DAYYANI, T., LEHMANN, C. and RAMOS, L., 2020. An Innovative Carbonate Facies Modeling Workflow That Honors Geological Concept, Case Study of Thamama. Abu Dhabi International Petroleum Exhibition & Conference, Abu Dhabi, UAE, November 2020, SPE-202805-MS. <https://doi.org/10.2118/202805-MS>
- AL-GHAMDI, N. and POPE, M., 2020. High-resolution Stratigraphic Architectures, Facies Anatomies of the Lower Cretaceous Biyadh and Shu'aiba Formations, and their Implications on Platform Evolution and Global Correlation. In: Khomsi, S. et al. (Eds), Arabian Plate and Surroundings: Geology, Sedimentary Basins and Georesources. Springer, pp 3-39. https://doi.org/10.1007/978-3-030-21874-4_1
- AL MANSOORI, A.I., STROHMENGER, C.J., GHANI, A.A.M.A. and MITCHELL, J., 2008. High-resolution sequence-stratigraphic correlation and facies characterization of Upper Thamama (Lower Cretaceous) reservoir units and non-reservoir zones, Abu Dhabi, United Arab Emirates. Abu Dhabi International Petroleum Exhibition and Conference, Abu Dhabi, UAE, November 2008, SPE-117905-MS, <https://doi.org/10.2118/117905-MS>
- ALSHARHAN, A. S., and SCOTT, R. W., 2000. Hydrocarbon potential of Mesozoic carbonate platform-basin systems, UAE. Middle East models of Jurassic/Cretaceous Carbonate Systems. *SEPM Special Publication* **69**, 335-358
- ARNAUD-VANNEAU, A., ARNAUD, H., COTILLON, P., FERRY, S. and MASSE, J.-P., 1982. Caractères et évolution des plates-formes carbonatées périvocotiennes au Crétacé Inférieur (France Sud-Est). *Cretaceous Res.*, **3**, 3-18
- AZER, S. and TOLAND, C., 1993. Sea level changes in the Aptian and Barremian (upper Thamama) of offshore Abu Dhabi, UAE: Society of Petroleum Engineers, paper SPE 25610, Proceedings of the Middle East Oil Show, pp 141-154.
- BARATA, J., VAHRENKAMP, V., VAN LAER, P.J., SWART P. and MURRAY, S., 2015. A regional analysis of clumped isotope geochemistry to define the timing of creation of microporosity in a lower Cretaceous giant reservoir. *Soc. Pet. Eng.* 177922, 10.
- BOICHARD, R.A.P., AL-SUWAIDI, A.S. and KARAKHANIAN, H., 1994. Sequence boundary types and related porosity evolutions: example of the upper Thamama Group in field "A" offshore Abu Dhabi, United Arab Emirates: 6th Abu Dhabi international petroleum exhibitions and conference. *Soc. Pet. Eng.* **76**, 191-201.
- BORGOMANO, J., MASSE, J.-P., and AL MASKIRY, S., 2002. The lower Aptian Shuaiba carbonate outcrops in Jebel Akhdar, northern Oman: Impact on static modeling for Shuaiba petroleum reservoirs. *AAPG Bulletin*, **86**(9), 1513-1529.
- BORGOMANO, J. R., FOURNIER, F., VISEUR, S. and RIJKELS, L., 2008. Stratigraphic well correlations for 3-D static modeling of carbonate reservoirs. *AAPG Bulletin*, **92**(6), 789-824.
- BORGOMANO, J., MASSONNAT, G., LANTEAUME, C., DANQUIGNY, C., SAMSON, P., ROLANDO J.P., and REBELLE M., 2020. Application of Stratigraphic Forward Modelling to Carbonate Reservoir Characterization – A New Paradigm from the Albion R&D Project. Abu Dhabi International Petroleum Exhibition & Conference, Nov 2020, Abu Dhabi.
- BOVER-ARNAL, T., SALAS, R., GUIMERA, J. and J.A. MORENO-BEDMAR, 2014. Deep incision in an Aptian carbonate succession indicates major sea-level fall in the Cretaceous: *Sedimentology*, **61**, 6, 1558-1593, doi:10.1111/sed.12105.
- CATUNEANU, O., ABREU, V., BHATTACHARYA, J.P., BLUM, M. D., DALRYMPLE, R. W., ERIKSSON, P. G. and WINKER, C., 2009. Towards the standardization of sequence stratigraphy. *Earth-Science Reviews*, **92**(1-2), 1-33.
- CARVALHO, A., DIAS, A. and RIBERIO, M., 2011. Oil recovery enhancement for Thamama B Lower in an Onshore Abu Dhabi Field. Using conceptual models to understand reservoir behaviour. SPE Reservoir Characterisation and Simulation Conference and Exhibition, October 2011, Abu Dhabi, UAE, SPE-148268-MS, <https://doi.org/10.2118/148268-MS>
- DAVIES, R.B., CASEY, D.M., HORBURY, A.D., SHARLAND, P.R.

- and SIMMONS, M.D., 2002. Early to mid-Cretaceous mixed carbonate siliciclastic shelfal systems: Examples, issues and models from the Arabian Plate. *GeoArabia*, **7**, 3, 541-598
- DEUTSCH, C.V. and WANG, L., 1996. Hierarchical object-based stochastic modeling of fluvial reservoirs. *Mathematical Geology*, **28**, 857-880.
- EHRENBERG, S. N., and WALDERHAUG, O., 2015. Preferential calcite cementation of macropores in microporous limestones. *Journal of Sedimentary Research*, **85**, 7, 780-793, <https://doi.org/10.2110/jsr.2015.52>
- EHRENBERG, S.N., MORAD, S., YAXIN, L. and CHEN, R., 2016. Stylolites and porosity in a Lower Cretaceous limestone reservoir, onshore Abu Dhabi. *Journal of Sedimentary Research*, **86**, 1228-1247. <https://doi.org/10.2110/jsr.2016.68>
- EHRENBERG, S.N., LOKIER, S.W., YAXIN, L. and CHEN, R., 2018. Depositional cycles in a Lower Cretaceous limestone reservoir, onshore Abu Dhabi, U.A.E. *Journal of Sedimentary Research*, **88**, 753-776. <https://doi.org/10.2110/jsr.2018.41>
- EHRENBERG, S.N., 2019. Petrophysical heterogeneity in a lower cretaceous limestone reservoir, onshore Abu Dhabi, UAE. *AAPG Bull.*, **103**, 527-546. <https://doi.org/10.1306/09061817298>
- EHRENBERG, S.N., ZHANG, J. and GOMES, J.S., 2020a. Regional porosity variation in Thamama-B reservoirs of Abu Dhabi. *Mar. Petrol. Geol.* **114**, 104245, <http://dx.doi.org/10.1016/j.marpetgeo.2020.104245>
- EHRENBERG, S.N., ZHANG, J. and GOMES, J.S., 2020b. Regional Variation of permeability in Thamama-B reservoirs of Abu Dhabi. *Mar. Petrol. Geol.* **116**, 104248, <http://dx.doi.org/10.1016/j.marpetgeo.2020.104248>
- EHRENBERG, S.N., NEILSON, J.E., GOMEZ-RIVAS, E., OXTOBY, N.H., JAYACHANDRAN, I.S.A.J, ADLAN, Q., and VAHRENKAMP, V. C., 2024, in press. Stratigraphy and diagenesis of the Thamama-B reservoir zone and its surrounding dense zones in Abu Dhabi oilfields and equivalent Oman outcrops, *Journal of Petroleum Geology*, **47**, 395-430.
- EVERTS, A.J.W., STAFLEU, J.A.N., SCHLAGER, W., FOUKE, B.W., and ZWART, E.W., 1995. Stratal patterns, sediment composition, and sequence stratigraphy at the margin of the Vercors carbonate platform (Lower Cretaceous, SE France). *Journal of Sedimentary Research* **B65**, 119-131.
- FENERCI-MASSÉ, M., MASSÉ, J.-P. and PERNARCIC, E., 2005. Quantitative stratigraphy of rudist limestones and its bearing on spatial organisation of rudist communities: the Late Barremian, Urgonian, sequences of Provence (S.E. France). *Palaeogeography, Palaeoclimatology, Palaeoecology* **215**, 265-284.
- FILBRANDT, J., S. AL-DHAHAB, A. AL-HABSY, K. HARRIS, J. KEATING, S. AL-MAHRUQI, S. OZKAYA, P. RICHARD and T. ROBERTSON, 2006. Kinematic interpretation and structural evolution of North Oman, Block 6, since the Late Cretaceous and implications for timing of hydrocarbons migration into Cretaceous reservoirs. *GeoArabia* **11**(1), 97-140.
- FOURNIER, F. and BORGOMANO, J., 2007. Geological significance of seismic reflections and imaging of the reservoir architecture in the Malampaya gas field (Philippines). *AAPG Bulletin* **91**(2), 235-258
- FRANCESCONI, A., BIGONI, F., BALOSSINO, P., BONA, N., MARTCHINI, F. and COZZI, M., 2009. Reservoir rock types application – Kashagan. Paper SPE-125342, Paper presented at the SPE/EAGE Reservoir Characterization Conference, Abu Dhabi, UAE, October 19–21, <http://dx.doi.org/10.2118/125342-MS>
- FRAU, C., TENDIL, A., POHL, A. and LANTEAUME, C., 2020. Revising the timing and causes of the Urgonian rudistid-platform demise in the Mediterranean Tethys. *Global and Planetary Change*, **187**, 103-124.
- GALLUCCIO, L., BREISLIN, C. and TENDIL, A., 2022. Capturing Reservoir Quality Heterogeneities at the Stage of Sedimentological Coding: an Innovative Depositional Environment Scheme. SPE-211662-MS. Abu Dhabi International Petroleum Exhibition and Conference. Society of Petroleum Engineers, <http://dx.doi.org/10.2118/211662-MS>
- GINSBURG, R. N., LLOYD, R. M., MCCALLUM, J. S., STOCKMAN, K.W. and MOODY, R. A., 1958. Surface sediments of Great Bahama Bank, Shell Development Company, Houston, Texas, USA.
- GRANIER, B., AL SUWAIDI, A.S., BUSNARDO, R., AZIZ, S.K. and SCHROEDER, R., 2006. New insight on the stratigraphy of the “Upper Thamama” in offshore Abu Dhabi (U.A.E.). *Carnets de Geologie* 2003, **(A05)**, 1-17.
- GROTSCH, J., AL-JELANI, O. and AL-MEHAIRI, Y., 1998. Integrated reservoir characterisation of a giant lower cretaceous oil field, Abu Dhabi, U.A.E. Abu Dhabi International Petroleum Exhibition and Conference, 11–14 November, Abu Dhabi, United Arab Emirates. Society of Petroleum Engineers Inc, <https://doi.org/10.2118/49454>
- HARRIS, P.M., PURKIS, S.J., ELLIS, J., SWART, P.K. and REIJMER, J. J., 2015. Mapping bathymetry and depositional facies on Great Bahama Bank. *Sedimentology*, **62** (2), 566-589.
- HARRIS, P., DIAZ, M. R. and EBERLI, G. P., 2019. The formation and distribution of modern ooids on Great Bahama Bank. *Annual Review of Marine Science*, **11**, 491-516.
- HILLGARTNER, H., VAN BUCHEM, F.S.P., GAUMET, F., RAZIN, P., PITTET, B., GROTSCH, J. and DROSTE, H. J., 2003. The Early Cretaceous carbonate margin of the eastern Arabian platform (northern Oman): Sedimentology, sequence stratigraphy and environmental change. *Journal of Sedimentary Research*, **73**, 756-773.
- IMMENHAUSER, A., 2009. Estimating palaeo-water depth from the physical rock record. *Earth-Science Reviews* **96**, 107-139.
- JEONG, J., AL-ALI, A.A., JUNG, H., ABDELRAHMAN, A., DHAFRA, A., SHEBL, H.T., KANG, J., BONIN, A., PERRIERE, M.D.D. and FOOTE, A., 2017. Controls on Reservoir Quality and Reservoir Architecture of Early Cretaceous carbonates in an Abu Dhabi Onshore Field Lekhwaib, Kharaib and Lower Shuaiba Formations: Abu Dhabi International Petroleum Exhibition & Conference, <https://doi.org/10.2118/188420-MS>
- KHAN, R., SALIB, M. S., BA HUSSAIN, A., BIN ABD RASHID, A., AYDINOGLU, G. and FAROOQ, U., 2018. Understanding the Influence of Structural Evolution Folding and Tilting on Hydrocarbon Accumulation Drainage and Imbibition and Reservoir Quality Diagenesis for Enhanced Field Development Planning, a Case Study of Lower Cretaceous Carbonate Reservoir, Abu Dhabi, UAE. 10.2118/193237-MS.
- LALLIER, F., CAUMON, G., BORGOMANO, J., VISEUR, S., FOURNIER, F., ANTOINE, C. and GENTILHOMME, T., 2012. Relevance of the stochastic stratigraphic well correlation approach for the study of complex carbonate settings: Application to the Malampaya build-up (Offshore Palawan, Philippines). *Geological Society of London Special Publication* **370**, 265-275.
- LANTEAUME, C., MASSONNAT, G., SAMSON, P., BORGOMANO, J., REBELLE, M., MICHEL, J. and DANQUIGNY, C., 2020. Carbonate Facies Models, Fake or Real? Comparison of the Urgonian Formation (south-east France) with the Kharaib-Shuaiba Formations (Middle East). 20 ADIP-P-3530-SPE
- LEONIDE, P., BORGOMANO, J., MASSE, J.P. and DOUBLET, S., 2012. Relation between stratigraphic architecture and multi-scale heterogeneities in carbonate platforms: The Barremian – lower Aptian of the Monts de Vaucluse, SE France. *Sedimentary Geology*, **265**, 87-109, <https://doi.org/10.1016/j.sedgeo.2012.03.019>
- LEONIDE, P., FOURNIER, F., REIJMER, J.J.G., VONHOF, H., BORGOMANO, J., DIJK, J., ROSENTHAL, M., VAM

- GOETHEM, M., COCHARD, J. and MEULENAARS, K., 2014. Diagenetic patterns and pore space distribution along a platform to outer-shelf transect (Urgonian limestone, Barremian – Aptian, SE France). *Sedimentary Geology*, **306**, 1–23, <https://doi.org/10.1016/j.sedgeo.2014.03.001>.
- MANGANE, P.-O., KENTNER, J., MECHELI, T., BORGOMANO, J. and NUSSBAUMER, C., 2024. *in press*. Reservoir Characterization in Carbonates: Rock Typing Strategy and Influence by Texture and Diagenesis. *AAPG Bulletin*, *in press*.
- MASSE, J.P., 1991. The Lower Cretaceous Mesogean benthic ecosystems: palaeoecologic aspects and palaeobiogeographic implications. *Palaeogeography, Palaeoclimatology, Palaeoecology* **91**, 331–345. [https://doi.org/10.1016/0031-0182\(92\)90075-G](https://doi.org/10.1016/0031-0182(92)90075-G)
- MASSE, J. P., BORGOMANO, J. and AL MASKIRY, S., 1997. Stratigraphy and tectonosedimentary evolution of a late Aptian – Albian carbonate margin: the northeastern Jebel Akhdar (Sultanate of Oman). *Sedimentary Geology*, **113** (3–4), 269–280.
- MASSE, J.P. and FENERCI-MASSE, M., 2011. Drowning discontinuities and stratigraphic correlation in platform carbonates: the late Barremian – early Aptian record of southeast France. *Cretaceous Research* **32**, 659–684. <https://doi.org/10.1016/j.cretres.2011.04.003>
- MATHERON, G., 1963. Principles of geostatistics. *Economic Geology*, **58** (8), 1246–1266.
- MELVILLE, P., AL JEELANI, O., AL MENHALI, S., GROTSCH, J., 2004. Three-dimensional seismic analysis in the characterization of a giant carbonate field, onshore Abu Dhabi, United Arab Emirates. In: Eberli, G.P., Massaferro, J.L. and Sarg, R.F. (Eds), *Seismic Imaging of Carbonate Reservoirs and Systems*. *AAPG Memoir* **81**, 123–148.
- MICHEL, J., LANTEAUME, C., MASSONNAT, G., BORGOMANO, J., TENDIL, A., BASTIDE, F., FRAU, C., LEONIDE, P., REBELLE, M., BARBIER, M., DANQUIGNY, C. and ROLANDO, J. P., 2023. Questioning carbonate facies model definition with reference to the Lower Cretaceous Urgonian platform (SE France Basin). *BSGF Earth Sci. Bull.* <https://doi.org/10.1051/bsgf/2023009>
- MOORE, C.H., 1989. Carbonate diagenesis and porosity. In: *Developments in Sedimentology*, **46**, Amsterdam, Elsevier. [https://dx.doi.org/10.1016/0920-4105\(92\)90066-A](https://dx.doi.org/10.1016/0920-4105(92)90066-A).
- PAGANONI, M., AL HARETHI, A., MORAD, D., MORAD, S., CERIANI, A., MANSURBEG, H., AL SUWAIDI, A., AL-AASM, I.S., EHRENBERG, S.N. and SIRAT, M., 2016. Impact of stylolitization on diagenesis of a Lower Cretaceous carbonate reservoir from a giant oilfield, Abu Dhabi, United Arab Emirates. *Sedimentary Geology*, **335**, 70–92.
- PITTER, B., VAN BUCHEM, F.S.P., HILLGARTNER, H., RAZIN, P., GROTSCH, J. and DROSTE, H.J., 2002. Ecological succession, palaeoenvironmental change, and depositional sequences of Barremian – Aptian shallow-water carbonates in northern Oman. *Sedimentology*, **49**, 555–581. <http://dx.doi.org/10.1046/j.1365-3091.2002.00460.x>
- POMAR, L., BASSANT, P., BRANDANO, M., RUCHONNET, C. and JANSON, X., 2012a. Impact of carbonate producing biotas on platform architecture: insights from Miocene examples of the Mediterranean region. *Earth-Science Reviews*, **113**, 186–211, doi: [10.1016/j.earscirev.2012.03.007](https://doi.org/10.1016/j.earscirev.2012.03.007).
- POMAR, L., AURELL, M., BÁDENAS, B., MORSILLI, M. and AL-AVWAD, S.F., 2015. Depositional Model for a Prograding Oolitic Wedge, Upper Jurassic, Iberian basin. *Marine and Petroleum Geology* **67**, 556–582. <https://doi.org/http://dx.doi.org/10.1016/j.marpetgeo.2015.05.025>
- PURKIS, S.J., VLASWINKEL, B. and GRACIAS, N., 2012. Vertical-to-lateral transitions among Cretaceous carbonate facies – a means to 3-D framework construction via Markov analysis. *Journ. Sediment. Res.*, **82**, 232–43
- PURKIS, S., KERR, J., DEMPSEY, A., CALHOUN, A., METSAMAA, L., RIEGL, B. and RENAUD, P., 2014. Large-scale carbonate platform development of Cay Sal Bank, Bahamas, and implications for associated reef geomorphology. *Geomorphology*, **222**, 25–38.
- PURKIS, S.J. and HARRIS, P.M., 2017. Quantitative interrogation of a fossilized carbonate sand body – the Pleistocene Miami oolite of South Florida. *Sedimentology*, **64**, 1439–64
- PURKIS, S.J., HARRIS, P. and CAVALCANTE, G., 2019. Controls of depositional facies patterns on a modern carbonate platform: insight from hydrodynamic modeling. *The Depositional Record*, **5**(3), 421–437.
- RANKEY, E.C. and REEDER, S.L., 2010. Controls on platform-scale patterns of surface sediments, shallow Holocene platforms, Bahamas. *Sedimentology*, **57**, 1545–1565.
- REBELLE, M., AL-NEAIMI, M., RIBEIRO, M. T., GOTTLIN-ZEH, S., VALSARDIEU, B. and MOSS, B., 2005. Quantitative and statistical approach for a new rock and log-typing model: Example of onshore Abu Dhabi Upper Thamama. (IPTC paper 10273.) International Petroleum Technology Conference, Doha, Qatar, 21–23 November 2005. <http://dx.doi.org/10.2523/10273-MS>
- SCHLAGER, W., 2005. Carbonate sedimentology and sequence stratigraphy. *SEPM Concepts in Sedimentology and Paleontology*, **8**. Society for Sedimentary Geology. <https://doi.org/10.2110/csp.05.08>
- SCOTT, R. W., 1990. Chronostratigraphy of the Cretaceous carbonate shelf, southeastern Arabia. *Geological Society of London Special Publication*, **49**, 89–108.
- SENA, C. N., JOHN, C. M. and COSGROVE, J. W., 2012. Integrated 3-D Sedimentological and Structural Study of a Lower Cretaceous Analogue Outcrop, Qishn Formation, Central Oman. In: *GEO 2012*. European Association of Geoscientists & Engineers, 2012. p. cp-287-00224.
- SHARLAND, P.R., ARCHER, R., CASEY, D.M., DAVIES, R.B., HALL, S.H., HEWARD, A.P., HORBURY, A.D. and SIMMONS, M.D., 2001. Arabian Plate Sequence Stratigraphy. *GeoArabia Special Publication* **2**, 371 pp.
- SHARLAND, P.R., CASEY, D.M., DAVIES, R.B., SIMMONS M.D. and SUTCLIFFE, O.E., 2004. Arabian Plate Sequence Stratigraphy - revisions to SP2. *GeoArabia*, **9**, 1, 199–214.
- SIMMONS, M.D., SHARLAND, P.R., CASEY, D.M., DAVIES, R.B. and SUTCLIFFE, O.E., 2007. Arabian Plate sequence stratigraphy: potential implications for global chronostratigraphy. *GeoArabia: Middle East Petroleum Geosciences*, **12** (4), 101–130.
- SKALINSKI, M., KENTER, J. and JENKINS, S., 2009. Rock type definition and pore type classification of a carbonate platform, Tengiz Field, Republic of Kazakhstan. *Proceedings of SPWLA 50th Annual Meeting*, June 21–24.
- STROHMENGER, C. J., WEBER, L.J. GHANI, A., AL-MEHSIN, K., AL-JEELANI, O., AL-MANSOORI, A., AL-DAYYANI, T., VAUGHAN, L., KHAN, S.A. and MITCHELL, J.C., 2006. High-resolution sequence stratigraphy and reservoir characterization of Upper Thamama (Lower Cretaceous) Reservoirs of a giant Abu Dhabi oil field, United Arab Emirates. In: *From Rocks to Reservoir Characterization and Modeling*. *AAPG Memoir* **88/SEPM Special Publication**, 139–171, <https://doi.org/10.1306/1215876M883271>
- TEILLET, T., FOURNIER, F., GISQUET, F., MONTAGGIONI, L.F., BORGOMANO, J., VILLENEUVE, Q. and HONG, F., 2019. Diagenetic history and porosity evolution of an Early Miocene carbonate buildup (Upper Burman Limestone), Yadana gas field, offshore Myanmar. *Mar. Petrol. Geol.* **109**, 589–606.
- TENDIL, A.J.-B., FRAU, C., LEONIDE, P., FOURNIER, F., BORGOMANO, J.R., LANTEAUME, C., MASSE, J.-P., MASSONNAT, G. and ROLANDO, J.-R., 2018. Platform-to-basin transition of the Urgonian carbonate platform in Provence (Barremian–Aptian, SE France): new insights into the regional to global factors controlling the local stratigraphic architecture. *Cretaceous Research*, **91**, 1–30.
- TENDIL, A., STUART, J., GALLUCCIO, L., BREISLIN, C.,

- AL-SHAMSI, S.G., SYOFYAN, S., AKI BAL BAHEETH, A.H., ADLAN, F., RAINA, I. and MANSOUR, B., 2022. Understanding Reservoir Heterogeneities in a Lower Cretaceous Thamama Reservoir. SPE-211678-MS, ADIPEC 2022, <http://dx.doi.org/10.2118/211678-MS>
- TUCKER, V., WRIGHT, P. and DICKSON, J.A.D., 1990. Carbonate Sedimentology. 482 pp., <http://dx.doi.org/10.1002/978144434175>
- VAHRENKAMP, V.C., 1996. Carbon isotope stratigraphy of the Upper Kharaib and Shuaiba Formations: implications for the Early Cretaceous evolution of the Arabian Gulf region. *AAPG Bulletin*, **80** (5), 647-661
- VAHRENKAMP, V.C., VAN LAER, P., FRANCO, B., CELENTANO, M.A., GRELAUD, C. and RAZIN, P., 2015. Late Jurassic to Cretaceous source rock prone intra-shelf basins of the eastern Arabian Plate – interplay between tectonism, global anoxic events and carbonate platform dynamics. In: International Petroleum Technology Conference, Doha, Qatar, 7-9 December, Paper IPTC-18470-MS, pp.24, <http://dx.doi.org/10.2523/IPTC-18470-MS>
- VAN BUCHEM, F.S.P., PITTET, B., HILLGARTNER, H., GROTSCH, J., AL MANSOURI, A.I., BILLING, I.M., DROSTE, H.H.J., OTERDOOM, W.H. and VAM STEENWINKEL, M., 2002. High-resolution sequence stratigraphic architecture of Barremian/Aptian carbonate systems in northern Oman and the United Arab Emirates (Kharaib and Shuaiba Formations). *GeoArabia* **7** (3), 461-500.
- VAN BUCHEM, F.S.P., AL-HUSSEINI, M.I., MAURER, F., DROSTE, H.J. and YOSE, L.A., 2010. Sequence-stratigraphic synthesis of the Barremian – Aptian of the eastern Arabian Plate and implications for the petroleum habitat. In: van Buchem, F.S.P., Al-Hussaini, M.I., Maurer, F., Droste, H.J. (Eds), *Aptian Stratigraphy and Petroleum Habitat of the Eastern Arabian Plate. GeoArabia Special Publication*, **4**, 9-48.
-